The Welfare Consequences of Urban Traffic Regulations

Isis Durrmeyer* Nicolás Martínez†

October 13, 2022

Abstract

We develop a structural model to represent individual transportation decisions, the equilibrium road traffic levels, and speeds inside a city. The model is micro-founded and incorporates a high level of heterogeneity: individuals differ in access to transportation modes, values of travel time, and schedule constraints; road congestion technologies vary within the city. We apply our model to the Paris metropolitan area and estimate the model parameters from publicly available data. We predict the road traffic equilibria under driving restrictions and road tolls and measure the policy consequences on the different welfare components: individual surplus, tax revenues, and cost of emissions.

JEL Classification: L9, R41, Q52

Keywords: structural model, policy evaluation, transportation, congestion, distributional effects, air pollution

*Toulouse School of Economics, Université Toulouse 1 Capitole and CEPR. E-mail: isis.durrmeyer@tse-fr.eu

†Toulouse School of Economics, Université Toulouse 1 Capitole. E-mail: nicolas.martinez@tse-fr.eu

We would like to thank Nano Barahona, Gaston Illanes, Luz Yadira Gómez-Hernández, Myrto Kalouptsidi, Nicolas Koch, Andrea Pozzi, Stef Proost, Valentina Reig, Mathias Reynaert, Marcelo Sant'Anna, and Xin Zhang for their helpful comments and suggestions. We would also like to thank the participants of various seminars and conferences. We acknowledge financial support from the European Research Council under grant ERC-2019-STG-852815 "PRIDISP" and Agence Nationale de Recherche under grant ANR-17-EUR-0010 (Investissements d'Avenir program).

1 Introduction

Road traffic reduction has been crucial in large metropolitan areas because of the multiple negative externalities cars generate. For instance, INRIX estimates an annual aggregate cost of congestion of 87 billion dollars for the U.S.[1] Pollution levels and air quality are also tightly related to the number of cars on the road. Yet, changes in road traffic level are difficult to predict because the road traffic level is the consequence of an equilibrium in which individuals make their transportation decisions independently. However, these individual decisions affect everyone since car speeds, and individual trip durations ultimately depend on the traffic level. Predicting individual reactions to a change in their transportation environment is challenging since it requires knowing how road traffic equilibrium is modified after individuals make their transportation decisions. Observational studies that measure the direct impact of a change in the transportation environment are limited by only being able to compare two equilibria, failing to separately identify the individual reactions from the equilibrium adjustments. We define transportation environment as all the factors that affect individual transportation decisions and are exogenous to individuals, including the presence of urban traffic regulations.

We develop a novel framework to analyze individual responses to changes in their transportation environments in equilibrium. It is a structural model representing equilibrium traffic conditions in a metropolitan area, with essential dimensions of heterogeneity at the individual and geographical levels. The first part of the model represents the choice of a transportation mode and a departure time by individuals with heterogeneous but fixed travel patterns (origin, destination, and itinerary). Since individuals have distinct travel patterns, different available transportation modes, and schedule flexibility, they are likely to react differently to a change in the transportation environment. Our model considers different transportation modes to be imperfect substitutes. We also account for possible schedule constraints, implying that individuals cannot substitute across departure times without utility loss. More precisely, we rely on a discrete choice nested logit model, containing heterogeneity in choice sets, sensitivities to trip duration, and preferences for the different departure times. The second part of the model represents the road congestion technologies, which describes how driving speeds react to changes in the number of individuals using cars and how many kilometers they drive. Our model takes into account spatial heterogeneity by allowing the road technology to be different across areas of the city.

The model has the advantage of being transparent, tractable, and estimable with combinations of data that are typically publicly available for many metropolitan areas. We also

[1] Source: https://www.cnbc.com/2019/02/11/americas-87-billion-traffic-jam-ranks-boston-and-dc-as-worst-in-us.html.

provide a methodology to verify whether the model parameters are such that the equilibrium is unique. This model differs from existing ones in three key aspects. First, the model represents equilibrium transportation decisions for the entire metropolitan area rather than focusing on a specific road. Second, it accounts for different types of roads with possibly different congestion technologies instead of considering one city-wide congestion technology. Third, all the model parameters are estimated and represent the joint distribution of preferences, trip distances and itineraries, individual characteristics, and transportation mode choice set, which is key to analyzing the effects of changes in the transportation environment at the individual level. To allow for such individual heterogeneity, we consider some factors are exogenous. In particular, we hold fixed residential locations and trip destinations, and we do not allow individuals to change where they live or work in response to a change in the transportation environment.[2] We also assume that the transportation modes available to an individual are fixed. While the choice of holding a car and the car characteristics (e.g., fuel efficiency) may be affected by traffic regulations in the medium run, we keep them constant in our analysis. Finally, we focus on unavoidable trips (work or study trips) and thus consider individuals who have to take their trips and do not model the number of trips.

We apply our model of transportation decisions and congestion to the Paris metropolitan area (Île-de-France region) and combine data from different sources to estimate the model parameters. We rely on a survey conducted in 2010 and 2011, where respondents provided detailed information about all the trips taken the day before the interview. We construct a final sample of 12,975 individuals to estimate the transportation mode choice model. The survey does not provide trip durations using the non-chosen alternative transportation modes or car trip durations for alternative departure times. We supplement the survey with data on expected travel times using Google Directions for public transport and TomTom application programming interfaces (API, hereafter) for private vehicles during peak and off-peak hours to overcome this issue. We estimate the congestion technologies using high-frequency data on traffic density and speed from road sensors at the day and hour level for 1,371 sensors covering the highways, the ring roads, and the city center. We also use subway and suburb train ridership data to approximate overcrowding levels in the different metro and train lines at peak and off-peak hours.

We use our structural model and estimated parameters to predict the effects of policy instruments that reduce road traffic. More specifically, we compare the effects of road tolls to simple driving restrictions. The advantage of driving restrictions is the simplicity of

[2]In our data, the first reason for choosing a residence is the price or size of the house (with 43.1% of respondents), while proximity to work and public transport come after (with 16.5% and 1.9% of respondents, respectively).

implementation, only requiring compliance controls and are often used as emergency schemes, temporary measures put in place under pollution peaks episodes.[3] Driving restrictions constitute a command and control policy instrument. An alternative consists of sending price signals through road tolls. Indeed, road tolls have been introduced in many European cities. For instance, Stockholm and London use systems of congestion charges, restricting access to the city center during peak hours of weekdays to those who pay a fee. Price mechanisms have the advantage of sorting individuals according to the benefits they get from driving: those who stop driving at peak hours have good transportation alternatives to driving or fewer schedule constraints, limiting the welfare costs of traffic regulations. Driving restrictions affect all individuals identically, which seems inefficient. In addition, road tolls generate tax revenue that can be redistributed to individuals, mitigating the surplus losses.

In the main analysis, we compare the effects of three simple policies: driving restrictions, fixed tolls, and variable tolls. The policies are restricted to peak hours, so we consider individuals free to drive during off-peak hours. First, we analyze the aggregate effects of different policy stringency levels. We find that all the regulations are costly for individuals, as speed gains cannot compensate for the losses from the constraints imposed by the policies. Under moderate stringency levels, both tolls improve aggregate welfare if their revenues are redistributed. From the aggregate consumer surplus perspective only, driving restrictions hurt individuals less than an uniform toll. They force everyone to contribute to the traffic reduction while tolls must be high to induce the same traffic reduction. Across tolls, the variable toll is more efficient than the uniform toll since it targets long-distance commuters, who exert the largest congestion externalities. However, the uniform toll is best at maximizing the tax revenue. These results indicate that the policymaker must arbitrage between different objectives. Next, we fix a stringency level and measure the policy costs and benefits. We find aggregate surplus losses between €0.7 million and €1.5 million per trip. We also measure the impacts of the policies on global pollutant emissions (carbon emissions, CO_2 hereafter) and local pollutant emissions: nitrogen oxide (NO_X), particulate matter (PM), and hydrocarbon (HC) emissions. The benefits from reducing emissions, computed using standard social values, compensate only between 2.4% and 4.5% of the surplus losses. We also go beyond the aggregate impacts of tolls and driving restrictions and analyze their distributional effects. The variable tolls generate the largest inequalities across individuals. Individuals with long-distance trips that do not have suitable public transport alternatives are most negatively impacted.

[3]Paris and the surrounding region have used alternate traffic restrictions based on license plate digits six times between 1997 and 2016. The longest alternate-day travel scheme lasted four days from December 6^{th} to 9^{th} 2016. Since 2017, emergency plans triggered due to pollution peaks have relied on targeted driving restrictions based on car vintage and fuel type combination.

Lastly, we investigate whether we can reduce surplus losses by using more sophisticated policy instruments or by combining policies with other interventions. We study a first-best benchmark where the policy maker sets personalized tolls to maximize welfare. Welfare gains are 63% larger and emissions reductions 27% larger than under the variable toll. However, the aggregate consumer surplus always decreases, and welfare improves because of the high tax revenues. We also study more realistic policies like car vintage or fuel-based driving restrictions, area-specific or combined variable and fixed tolls, and driving licenses allocated through an auction. These instruments do not perform significantly better than the simple ones for surplus losses and emission reductions. We also measure the potential gains from differentiated tolls according to the area and nonlinear variable tolls. Finally, we evaluate the role of access to public transport, public transport efficiency, and cost for surplus losses. We find that connecting the 28.5% of the population which currently does not have access to public transportation and improving public transport speed are the best ancillary instruments to reduce policy surplus losses.

Barwick et al. (2021) estimate a model that is the most similar to ours to analyze the impact of tolls and driving restrictions on commuting choices and equilibrium congestion levels in Beijing. In addition, they endogenize individual housing location decisions and investigate the policies' effects on residential sorting. To do so, they rely on rich individual data that include housing prices and characteristics, household characteristics, and individual work locations. Their model endogenizes the residential location, which we consider fixed in our model. However, they have a more restrictive representation of the congestion technology in the city since they assume a single congestion technology with a constant speed elasticity.

Kreindler (2022) also estimates a structural model of transportation decisions to analyze the welfare effects of congestion pricing in India. He leverages experimental data to estimate departure time substitution patterns and price sensitivity. His model differs from ours in several aspects: it includes separate costs for being early, late, or spending time in traffic (in the spirit of traditional bottleneck models) and allows for substitution across routes rather than transportation modes. Tarduno (2022) develops a structural model of transportation decisions with route and departure time substitution for a bridge in San Francisco metropolitan area in the U.S. His results highlight the importance of accounting for policy leakage, i.e., route substitution, and he characterizes the second-best tolls that account for it. However, his model is quite different from ours since he abstracts from mode substitution, does not model the congestion technology, and ignores the effects of individual decisions on equilibrium speeds.

We relate and extend the transportation literature linking individuals' decisions and

congestion. For instance, Basso and Silva (2014) model the choice between driving and taking the bus and the substitution between peak and off-peak hours over a single road to compare the effectiveness of public transport improvements and road tolls. Like in our model, both periods are associated with different congestion levels that depend on car and bus usage. However, the approach is different since they calibrate the model and ignore other transportation modes. Batarce and Ivaldi (2014) estimate a mode choice model with endogenous congestion based on the number of individual trips. Driving at any point in time generates congestion for the whole day.

Other empirical models that represent transportation decisions and congestion are based on the bottleneck model of Arnott et al. (1990) and Arnott et al. (1993). These models have the advantage of carefully describing congestion dynamics for a single road but ignore the substitution between driving and other transportation modes. Indeed, Anderson (2014) shows that the substitution between cars and public transport significantly affects congestion levels. Van Den Berg and Verhoef (2011) and Hall (2021) use bottleneck models to measure the distributional effects of road tolls. Both studies show that congestion pricing can improve consumer surplus without toll revenue redistribution due to sorting individuals according to their value of travel time. We find that road tolls never increase the total consumer surplus without redistributing the toll revenue like Barwick et al. (2021) and Kreindler (2022), who make similar assumptions to ours. One reason for finding adverse effects of road tolls on consumer surplus is that we model traffic level at the period level instead of using a continuous time measure, ignoring the sorting of individuals within the period. Furthermore, we consider all roads tolled while Hall (2018) and Hall (2021) consider policies that price a fraction of the roads.

The methodology of our paper relies on standard methods to estimate substitution patterns between transportation modes and departure times. Discrete choice models have indeed a long tradition of being used to model transportation mode choices (McFadden, 1974, Small, 2012) and estimate the value of travel time (VOT). Recent literature has relied on new data to estimate the VOT. For instance, Small et al. (2005) estimates individuals' VOT and valuations of travel time reliability using a mix of revealed and stated preferences data. Bento et al. (2020) use data from drivers entering an expressway subject to a toll in Los Angeles to disentangle the value of urgency from the VOT of individuals, highlighting the role of schedule constraints on individuals' willingness to pay for road tolls. Buchholz et al. (2020) exploits data from a ride-sharing platform to retrieve individuals' VOT. They exploit variations in prices and waiting times to recover the distribution of VOT in the population. Recent work have implemented field experiments to elicit directly travel time valuations (Kreindler, 2022, Goldszmidt et al., 2020, Hintermann et al., 2021). Our estimates of the

VOT rely much more on the model structure since we rely on standard cross-sectional survey data. Our estimates are nevertheless consistent with the estimates from this literature.

Our reduced-form model for the congestion technology extends the work from the literature in two ways. First, we do not impose a linear relationship between speed and traffic density as in Russo et al. (2021), Yang et al. (2020), Couture et al. (2018), Akbar and Duranton (2017). We estimate the relationships between speed and traffic density flexibly and find that the marginal impact of traffic on speed is not constant. Second, we do not assume a single congestion level for the whole city. Instead, we estimate five area-specific congestion technologies and model the equilibrium traffic level in each area and each period. Both differences from the standard literature have an important consequence: the marginal cost of congestion varies with the traffic level and the city area.

This paper relates to the literature measuring the impacts of existing traffic regulations using direct policy evaluation methods. The initial literature focused on developing countries with long traditions of urban traffic policies. Davis (2008), and Gallego et al. (2013) show that driving restrictions reduce pollution in the short run but are harmful in the long run because individuals bypass the restriction by purchasing a second car. Recent studies evaluate European policies such as low emissions zones, congestion charges, and road closures (Galdon-Sanchez et al., 2021, Tassinari, 2022, Herzog, 2022, Bou Sleiman, 2021). Our analysis is different in terms of method and focus. First, we evaluate hypothetical policies. Second, we analyze the heterogeneity of the policy effects across individuals and their distributional consequences. We can also provide estimates for unobserved outcomes that can be expressed as a function of the model parameters, like consumer surplus. Previous literature on urban traffic policies in Paris (De Palma and Lindsey, 2006, Kilani et al., 2014) models the equilibrium traffic level with a less detailed characterization of individual preferences and limited mode substitution. The Metropolis model (De Palma et al., 1997) incorporates a version of the bottleneck model into a calibrated citywide traffic simulator for the Paris metropolitan area. However, this model relies on external parameters. One advantage of our framework is that all parameters are estimated, and the model equations are transparent. De Palma et al. (2017) and Haywood and Koning (2015) study the role of public transport quality in Paris for driving decisions. These studies focus on specific subway lines and ignore alternative transportation modes.

Our analysis is related to spatial equilibrium models interested in the locations of individuals and activities and the role of transportation policies. For instance, some recent papers has focused on infrastructure improvements and transportation policies (see Allen and Arkolakis, 2022, Tsivanidis, 2022, Herzog, 2022). Carstensen et al. (2022) model the residential and

work location choices and how they are affected by a distance-based commuting cost in a dynamic framework. While our model is very different from these general spatial equilibrium models, some results from our paper could be useful for this literature to account for traffic condition adjustments.

2 A structural model of transportation decisions and traffic conditions

We develop an equilibrium model representing individual choice of a transportation mode and departure time. The model considers that car trip durations are endogenous and depend on the congestion levels on the roads which is directly related on the number of drivers and how long they spend on the road. We approximate this by the number of kilometers individuals drive at each time period. To represent the relationship between speed and traffic density, we model road congestion technologies for different metropolitan areas. Finally, we describe how to solve for the equilibrium of the model and check whether the equilibrium is unique.

2.1 Transportation mode choice model

First, we introduce the structural model representing how individuals decide which transportation mode to use and their departure time. We consider that the origin and destination of the trips are fixed and exogenous. We do not allow for an outside option, as we model the choice of individuals facing non-avoidable trips. We make the simplification that individuals choose between T periods denoted by $1, ..., T$. Our model is a nested discrete choice model, and we follow the standard distributional assumptions from the literature (see, Train, 2009). The nests are the different transportation modes. We assume individuals make a sequential decision: first, they choose a transportation mode, and then they decide when they leave. The consequence of this modeling assumption is that we allow individuals to have correlated preference shocks for the same transportation mode across departure periods. The utility function of an individual n associated with transportation mode j, and departure time t is assumed to be linear in the mode and departure period characteristics X_{njt} (which include the trip cost, trip duration and mode and period specific intercepts):

$$u_{njt} = \beta_n' X_{njt} + \epsilon_{njt}.$$

β_n is a vector of coefficients of preferences for these variables for consumer n, and ϵ_{njt} is a random idiosyncratic term. This assumption implies that the different modes and departure periods are imperfect substitutes. We allow for correlation between these idiosyncratic terms

across different periods by decomposing the preference shocks into a mode-specific shock common to all departure periods and a mode and period-specific shock:

$$\epsilon_{njt} = \zeta_{nj} + \sigma\tilde{\epsilon}_{njt}.$$

σ represents the degree of independence between the preference shocks across different periods for the same transportation mode and is a parameter to estimate. When $\sigma = 1$, the preference shocks for different periods are independent, while if $\sigma = 0$, the different time periods are perfect substitutes. We assume that the period-specific preference shocks share the same correlation coefficient. Distant periods might be less substitutable than closer ones; our model captures this through the mode and period-specific constants that should be more similar. Each individual has a choice set $\mathcal{J}_n$, which comprises all transportation modes she can access. Each individual chooses the combination of alternative j^* and departure time t^* that maximizes their utility:

$$\{j^*, t^*\} = \underset{j\in\mathcal{J}_n, t\in\{1,\dots,T\}}{\arg\max}\ u_{njt}.$$

We assume that ϵ_{njt} are identically and independently distributed across individuals and follow a type one extreme value distribution. We further assume that the preference shocks are uncorrelated to the mode and period observed characteristics:

$$\mathbb{E}(\epsilon_{njt}|X_{njt}) = 0.$$

The probability that individual n chooses the transportation mode j and departure time t is:

$$s_{njt} = \frac{\exp\left(\frac{\beta_n' X_{njt}}{\sigma}\right)}{D_{nj}^{1-\sigma}\sum_{j'\in\mathcal{J}_n} D_{nj'}^{\sigma}},$$

where $D_{nj'} = \sum_{t=1}^{T}\exp\left(\frac{\beta_n' X_{nj't}}{\sigma}\right)$. In our data, we observe a sample of N individuals, who are representative of the entire population in the metropolitan area using the individual weights. By aggregating the transportation mode decisions of all individuals, we obtain the total number of individuals using transportation mode j at period t as:

$$N_{jt} = \sum_{n=1}^{N}\omega_n s_{njt},$$

where ω_n is the weight of individual n in the sample. We can also obtain the total number of kilometers driven in a given period as:

$$K_t = \sum_{n=1}^{N} \omega_n k_n s_{nt,\text{car}}.$$

For the estimation, we further parameterize the individual heterogeneity in preferences and assume that β_n are functions of observable demographics characteristics Z_n:

$$\beta_n = \bar{\beta} + Z_n \Gamma$$

We estimate $\left(\bar{\beta}, \Gamma, \sigma\right)$ using the method of maximum likelihood; we want to find the values of the parameters that rationalize the best the observed choices given the theoretical probabilities. The log-likelihood function that we maximize is:

$$LL(\bar{\beta}, \Gamma, \sigma) = \sum_{n=1}^{N} \sum_{j \in \mathcal{J}_n, t \in \{1,...,T\}} \omega_n d_{njt} \times \log\left(s_{njt}(\bar{\beta}, \Gamma, \sigma)\right), \tag{1}$$

where d_{njt} is an indicator equal to one when the transportation mode j and time t are chosen and zero otherwise. ω_n corresponds to the sample weight of the individual n. The identification of the parameters comes from observing a cross-section of individuals who have different choice sets, different trip characteristics, and different demographic characteristics.

2.2 Road traffic conditions and congestion technology

We model congestion technology at the local level, splitting the city in $a = 1, ..., A$ mutually exclusive areas. The driving speed in an area depends on the road technology and the traffic density in that area only. Following the transportation literature, we base our congestion technology model on the fundamental traffic diagram (see Small et al., 2007). We model speed as a weakly decreasing function of the traffic density, represented by the occupancy rate that traffic monitoring stations typically record. The occupancy rate is defined as the percentage of a fixed period during which the traffic sensor detects a car. Geroliminis and Daganzo (2008) empirically show the existence of a fundamental traffic diagram at the city level, called a "macroscopic fundamental traffic diagram". Other applications include Yang et al. (2020), Couture et al. (2018), and Anderson and Davis (2020). We follow their approach but allow for heterogeneity within the city by considering area-specific congestion technologies. We also rely on minimal functional form assumptions by approximating the function by polynomials.

Congestion levels can be different throughout the day, but we consider that road technology is fixed over time. Road technology represents all the elements that determine the speed

at which individuals can drive for a given traffic density. It represents the type of road (high-speed road or city road), the presence of traffic lights and intersections, and the number of entries or exits that may force drivers to slow down. Formally, we define the speed in area a at time t, v_t^a to be a function of the occupancy rate τ_t^a:

$$v_t^a = f^a(\tau_t^a)$$

f^a represents the congestion technology, which indicates how the speed decreases when the number of cars increases. For the estimation, we consider that the observations contain speed shocks such that:

$$v_t^a = f^a(\tau_t^a) + \nu_t^a.$$

We assume that the speed shocks are exogenous and uncorrelated to the traffic level τ_t^a. We make minimal function form assumptions on f^a by relying on basis polynomial. More specifically, we use Bernstein basis polynomials. We observe a sample of independent realizations of traffic densities and speeds and estimate the following equation:

$$v_t^a = \sum_{l=0}^{L} c_l^a B_l(\tau_t^a) + \nu_t^a.$$

The coefficients c_l^a are the parameters of interest, and B_l are the Bernstein basis polynomials of degree L, which expressions are:

$$B_l(\mathcal{T}) = \binom{L}{l} \mathcal{T}^l (1-\mathcal{T})^{L-l}.$$

Under the assumption that the occupancy rate τ_t^a is independent of the speed shock ν_t^a, we can estimate the parameters of the Bernstein polynomial c_l^a using standard linear methods.

The congestion technology model determines speeds from the traffic occupancy rates, while the transportation mode choice model predicts the number of cars and the number of kilometers driven by area. We thus need to map the number of kilometers predicted by the transportation mode choice model and the average occupancy rate in each area. Because the traffic level depends on how many individuals choose to drive and how long they drive, we consider a mapping between the total number of kilometers driven and the occupancy rate. We assume an affine relation between the occupancy rate and the total number of kilometers driven at the area level. Because we do not model the entire traffic source, we let the possibility that a fraction of the road traffic is irreducible (trucks, delivery cars, buses, etc...). Formally, we consider:

$$\tau_t^a = \phi_t^a \times K_t^a + \gamma_t^a,$$

where ϕ_t^a is a scale parameter that maps the number of kilometers driven to the surface of the area, and γ_t^a represents the irreducible traffic.

2.3 Equilibrium of the model

In this model, an equilibrium is defined by individual probabilities to drive at each period and speeds for each area and period. Then, we substitute the individual probabilities in the speed function to express the equilibrium in terms of speeds only and get the following system of non-linear equations:

$$v_t^a = f^a\left(\phi_t^a \sum_{n=1}^{N} \omega_n . s_{nt}(\mathbf{v}) . k_n^a + \gamma_t^a\right)$$

There is no general result that guarantees that the system of non-linear equations always has a unique solution. However, there are two special cases where the speed equilibrium is unique. The first particular case is when there is only one period and one area, so we have just a non-linear equation to solve. Because the speed function f^a is monotonically decreasing, we are sure that if a speed equilibrium exists, it is unique. The second particular case is when we have one area and multiple periods. The proof relies on the fact that the Jacobian of the system of equations has positive terms on the diagonal and negative terms off-diagonal. The property of the Jacobian of the system of equations is the consequence of two key features of our model: the speed function is decreasing, and the different departure periods are substitutes. We provide the proofs of uniqueness under these two particular cases in Appendix A.1. Even though there is no proof of the uniqueness of the equilibrium, we provide a method to check if the system of equations in speeds has a unique solution given our set of estimated parameters. The approach consists of defining the function:

$$g_t^a(\mathbf{v}, \kappa) = \kappa . v_t^a + (1 - \kappa) . f^a(\mathbf{v})$$

and check whether there exists $\kappa \in [0, 1[$ such that $\mathbf{g}(.) = \left(g_1^1 \cdots g_T^1 \cdots g_1^A \cdots g_T^A\right)'$ is a contraction. Recall that a function $\mathbf{g}(.)$ is a contraction if it is K-Lipschitz, with $K<1$, implying that $\forall \mathbf{v} \in [\underline{\mathbf{v}}, \overline{\mathbf{v}}]$:

$$||\mathbf{g}(\mathbf{v}') - \mathbf{g}(\mathbf{v})|| \leq K||\mathbf{v}' - \mathbf{v}||.$$

We use the supremum norm, so the Lipschitz coefficient K is given by:

$$\max_{a\in 1,\dots A}\max_{t\in 1,\dots,T}\max_{a'\in 1,\dots A}\max_{t'\in 1,\dots,T}\max_{\mathbf{v}\in[\underline{\mathbf{v}},\overline{\mathbf{v}}]}\left|\frac{\partial g_t^a(\mathbf{v},\kappa)}{\partial v_{t'}^{a'}}\right|.$$

Suppose we can find $\kappa \in [0,1[$ such that $K<1$, the function $\mathbf{g}(.)$ is a contraction. Therefore, if the iteration process converges, it converges to the unique solution of the system of equations. If there exists a set of κ such that the function $\mathbf{g}(.)$ is K-Lipschitz with $K<1$, then we select the value of κ that implies the lowest coefficient K to ensure the maximum speed of convergence. Therefore, we solve for:

$$\min_{\kappa\in[0,1[}\max_{a\in 1,\dots A}\max_{t\in 1,\dots,T}\max_{a'\in 1,\dots A}\max_{t'\in 1,\dots,T}\max_{\mathbf{v}\in[\underline{\mathbf{v}},\overline{\mathbf{v}}]}\left|\frac{\partial g_t^a(\mathbf{v},\kappa)}{\partial v_{t'}^{a'}}\right|.$$

We provide in Appendix A.2 the analytical formula for the Jacobian of $\mathbf{g}(.)$, and in Appendix C.4 some results on how the Lipschitz coefficient varies with the tuning parameter κ and the policy environment.

3 Specification and estimation of the transportation choice model

We estimate the transportation choice model parameters using a combination of two main datasets. We rely on survey data on individual commuting patterns in the Paris area called "Enquête Globale Transport 2010" (EGT hereafter). It is combined with a second self-constructed dataset on expected trip durations and itineraries for cars and public transport from TomTom and Google Maps APIs. We also leverage several ancillary datasets to complement the information on the different transportation modes and individual characteristics. We present all the sources for the data in Appendix B.1.

3.1 Data, sample selection and choice set characteristics

The EGT data contain information about departure times, precise locations, transportation mode for every trip, and trip motives. In addition, the survey records household and individual socio-demographic characteristics such as age, socio-professional activity, household size, income class, and housing characteristics. We model the choice of transportation mode and departure period for the morning commute, and consider two time periods: peak and off-peak hours. We assume individuals choose only one mode of transportation. If individuals take

multiple modes, we keep the one reported as the primary mode.[4] To focus on transportation decisions that are non-avoidable, we restrict the sample to trips related to work or study motives. However, we still cover a large share of transportation decisions as non-avoidable trips represent 73.1% of the total distance traveled between 7:00-8:59 a.m. and 69.5% for the period between 6:00-6:59 a.m. and 9:00-9:59 a.m. We pick the individual as the observation unit rather than the household, assuming that individual decisions are independent within families; individuals from the same home still share access to the same transportation modes and household demographic characteristics. This assumption implies that two people can take the same car to make their respective trips; in this case, we consider two vehicles are on the road. [5] While this simplification ignores potential cost savings and detours associated with carpooling, modeling such joint decisions would add too much complexity to the model. We consider five transportation mode alternatives: bicycle, public transport, two-wheeled motor vehicles (motorcycle), walking, and car.[6] If the household does not own a car or a motorcycle, the alternative is considered unavailable for the individual. If walking or biking takes more than 2.5 hours, we also define those alternatives as unavailable. If Google Maps cannot provide a public transport itinerary, we consider the option unavailable (this occurs for 28.5% of the sample). We obtain a final sample of 12,975 individual trips. With the sample weights, we have transportation decisions representing 4,034,801 individuals, corresponding to approximately one-third of the total population of the Paris metropolitan area (11.9 million inhabitants in 2011). Our entire analysis uses the survey weights to provide results for the professionals and students from kindergarten in the Paris metropolitan area.

Since the EGT data only provide trip durations for chosen transportation modes, we must rely on additional data to compute travel times. For consistency across alternatives, we ignore self-reported trip durations. Instead, we consider travel times that we generate for chosen and non-chosen transportation modes. We use Google Maps API to provide expected trip durations and itineraries by public transport and use TomTom API for expected driving times. We specify the trip query to a future date, so the predictions are not subject to the current traffic conditions and their idiosyncrasies. The predictions nevertheless rely on the expected traffic level to predict car trip durations. We thus use the predicted car trip durations at 8:30 a.m. for peak hours and 6:30 a.m. for off-peak hours. We provide more details about the queries in Appendix B.1. To estimate durations for walk and bicycle trips, we obtain the trip distances from the walking route itinerary given by Open Source Routing

[4] Only 8.2% of public transport trips also used a car, and less than 1% a bicycle or motorcycle.

[5] In our sample, only 6.7% of the individuals report using a car as a passenger.

[6] Recent literature highlights the role of ridesharing and taxis on congestion levels (Rosaia, 2020 and Mangrum and Molnar, 2020). For the EGT survey period, ridesharing is not an available alternative. Furthermore, only 0.17% of the trips were done using a taxi, which is why we ignore the alternative.

Machine.[7] Then, we compute the average speed for individuals who bike and walk using their declared trip durations and the distance. We find a walking speed of 5.52 km/hr and 10.23 km/hr for biking.[8] The average speeds and the recovered distances are then used to compute trip durations for the two modes. Finally, we use the predicted car durations at off-peak hours for motorcycles, assuming they can bypass traffic.

The EGT data contains information on some characteristics of cars and motorcycles. Using additional data, we estimate the fuel consumption per kilometer driven and the emissions for the vehicles from these characteristics (see Appendix B.2). Fuel consumption is essential to estimate the cost of driving, while the emissions are helpful in the counterfactual simulations to predict the environmental policy effects. The survey also records whether individuals own a public transport pass, the type of subscription and if they are partly or entirely reimbursed for their trip. Using this information and additional assumptions, we estimate the costs for each available transportation mode for all individuals. We construct cost estimates consistent with marginal costs rather than average costs. Thus, we ignore fixed costs such as the cost of the car, annual insurance, or parking. Following Hang et al. (2016), we do not include vehicle depreciation in our cost estimates either. Finally, we assume biking costs are zero when individuals own a bicycle. Otherwise, we attribute the price of a bike sharing ticket (€1.7). Our final cost estimates are trip and individual-specific and account for differences in the public transportation subscriptions, vehicle characteristics, and trip distances. We provide the precise methodology and related assumptions to estimate the costs in Appendix B.3.

We construct a measure of overcrowding for all the subway and urban railway transit lines to capture the potential disutility of overcrowding in public railway transport. We use publicly available data from 2015 on passenger flows (the oldest year available) combined with data on hourly public transit schedules and train capacities. A train's capacity is the number of passengers in a train for a density of four persons per square meter. We approximate the overcrowding level by the ratio between the hourly number of passengers divided by the line's capacity. This variable reflects the time heterogeneity in train passenger flow, schedules, and capacities. From the urban railway line-level overcrowding estimates, we obtain individual overcrowding levels by weighting the line-level overcrowding measures by the percentage of the trip duration spent on the line. We provide details on the data used and the construction of the overcrowding variable in Appendix B.4. On average, we find that the public railway transport is at 89% capacity at off-peak hours and reaches 143% at peak hours.

[7] Source: http://project-osrm.org/

[8] We check that the speeds are not sensitive to rounding errors in the reported trip durations by excluding observations reporting a multiple of 5 minutes and the average speeds remain very similar.

The survey only provides household income brackets, dividing the full income distribution in ten brackets. We prefer to construct our own proxy of household wealth by leveraging precise housing size and location information. We estimate the real estate value per square meter in each household's neighborhood using estate transaction data from the French tax authority. The real estate prices are estimated using all transactions in the municipality and the neighboring municipalities and weighting each match by the inverse of the distance to the household's location. We then multiply this estimate by the apartment or house size observed in the EGT data. Finally, we divide our estimated household wealth by the number of consumption units in the household. According to the French Statistical Institute (INSEE), the first individual in a household represents one consumption unit, other adults represent half a consumption unit, and children represent 0.3 consumption units. We provide more details about the data and estimates in Appendix B.5. We find a correlation coefficient of 0.51 between our income proxy and the midpoints of the income bracket provided by the EGT data.

Table 1: Summary statistics by demographic groups.

		Mean		Mode shares			
	Freq.	**Distance**	**Duration**	**Car**	**Peak/ car chosen**	**PT**	**Peak/ PT chosen**
Age							
Age $\leq$ 18	25.4	4.21	18.9	21.3	93.7	31.8	81.7
Age $\in$]18- 25]	10.8	14.8	38.9	20.6	57.4	68.9	62.5
Age $\in$]25- 35]	17.8	15.5	35	36.7	57.6	52.7	66.6
Age $\in$]35- 45]	19.4	17	35.6	45.7	57.9	43.2	62.1
Age $\in$]45- 60]	24	16.5	34.9	45.3	63.5	43.9	65.9
Age $>$ 60	2.56	13.4	30	49.9	56.1	39.7	64.6
Wealth proxy							
Wealth $\leq$ 110,000	20	14.6	32.8	36.7	57	41.3	58.3
Wealth $\in$]110,000-152,000]	20	14.9	33.2	39.5	65.1	42.7	64.8
Wealth $\in$]152,000-205,000]	20	13.4	31.8	37.2	65.3	44	69.7
Wealth $\in$]205,000-283,000]	20	12	30.2	33.7	68.4	47.7	71.1
Wealth $>$ 283,000	20	10.1	28.5	28.8	70.8	48.6	72.7
Socio-professional category							
Independent	3.58	17	30.5	59.5	51.8	24.4	61
White collar	33.3	15.9	35.2	39.3	70.5	49.6	74.5
Blue collar	30.6	16.4	35.3	44.5	50.2	45.2	54.4
Student $\leq$ high school	25.6	4.09	18.8	21.6	93.3	31.5	82.8
Student - higher education	6.86	15.1	41.9	11.7	68.1	80.4	58.8
Household size							
Couple and/or children	84	13.1	31.2	35.6	65.9	42.9	68.6
Single	16	12.7	32.2	32.9	60.2	55.1	63.8
Average		13	31.3	35.2	65	44.8	67.6

Note: Durations in minutes, distances in km, wealth in € per household consumption unit. Frequencies and mode shares are in %. Distance and duration are those of the chosen transportation modes.

Table 1 shows the distribution of trip characteristics and mode shares across the different demographic categories. We see that the youngest category (younger than 18 years old)

have, on average, trip distances three to four times lower than the rest of the population. The explanation is the proximity of schools to their residences. We do not observe large differences in car usage for the first three wealth quintiles. Instead, there is considerably lower usage for the top two quintiles. We see that the share of individuals using public transport and traveling at peak hours increases with wealth. While the share of white-collar workers using their car differs by 5.2 percentage points from the share of blue-collar workers, the percentage of white-collar workers driving at peak hours is 19.7 percentage points higher than for blue-collar workers. We take this as evidence of differences in schedule flexibility across socio-professional categories. Mode availability, as well as the distribution of durations and costs by mode, are given in Appendix B.6.

3.2 Model specification and estimation results

We specify the utility as a linear function of the following variables: transportation mode-specific intercepts, the trip's monetary cost, and the logarithm of the trip duration. Only differences in utilities are identified in these discrete choice models, so we consider walking as the baseline option and normalize the intercept to 0. Note that the mean utility of walking is not normalized to 0 because the utility contains the trip duration. We use the logarithm of the trip duration since it implies that the marginal valuation of travel time decreases with the trip duration: spending one additional minute is more harmful to someone taking a short trip than to someone with a longer trip time. We test in robustness the sensitivity of the results to this specification assumption. We allow the sensitivity to the trip duration to vary with age (we rely on six age classes) and wealth (we rely on the quintiles of our wealth proxy). The trip duration might be differently valued if individuals have to make a physical effort or if they can use their time to read or listen to the radio. To capture this, we add an interaction between a dummy for walking and bicycle and the trip duration in the utility function. While we allow for heterogeneity in the sensitivity to the trip duration, we do not allow heterogeneity in the cost sensitivity. We choose to put all the heterogeneity on the sensitivity to the duration for two reasons. First, the trip durations are fairly precisely measured, while the trip cost estimates rely on several assumptions and imputations. Second, the costs display much less variation across modes and individuals than trip durations. We also test this restriction in a robustness exercise.

Individuals may have different schedule flexibility. Workers in some specific professional activities and young students may have less departure time flexibility. Therefore, we interact the socio-professional category with a dummy for off-peak hours. Families typically try to coordinate departure times and may be less flexible, so we also add an interaction between an indicator for families and off-peak hours.

Additionally, we add some controls to represent the characteristics of public transport. We use the overcrowding level in the metro and suburb trains, a dummy if the public transport itinerary relies on the railway system only (instead of using the bus or tramway), and the number of layovers. Following the literature on public transport congestion, such as De Palma et al. (2017) and Haywood and Koning (2015), we assume the utility is linear in the level of overcrowding in the public transit.

Table 2: Estimation results for the utility parameters

Coefficients	**Mean**	**S.E.**
Log(duration)	-0.56**	0.09
Log(duration) × wealth ∈ q2	-0.05	0.08
Log(duration) × wealth ∈ q3	-0.01	0.08
Log(duration) × wealth ∈ q4	-0.11	0.08
Log(duration) × wealth ∈ q5	0.15†	0.09
Log(duration) × age ∈]18-25]	-0.4**	0.1
Log(duration) × age ∈]25-35]	-1.59**	0.09
Log(duration) × age ∈]35-45]	-1.7**	0.08
Log(duration) × age ∈]45-60]	-1.45**	0.08
Log(duration) × age > 60	-2.03**	0.2
Log(duration) × effort	-1.66**	0.06
Cost	-0.41**	0.02
Bicycle	-3.48**	0.08
Public transport, peak	-4.2**	0.21
Public transport, off-peak	-4.49**	0.23
Motorcycle	-7.35**	0.21
Car, peak	-6.22**	0.2
Car, off-peak	-6.81**	0.22
Off-peak hour × white collar	-0.57**	0.09
Off-peak hour × blue collar	0.16†	0.08
Off-peak hour × student ≤ high school	-0.98**	0.12
Off-peak hour × student > high school	0.01	0.1
Off-peak hour × family	-0.08†	0.04
No. layovers in public transport	-0.35**	0.04
Railway only	0.05	0.06
Public transport overcrowding	-0.06**	0.02
σ	0.79**	0.06
No. observations	12,975	
Log-likelihood	-13,624	

*Notes: Walk is the baseline alternative. The reference categories are individuals with age < 18, the first wealth quintile and independent workers. Duration measured in minutes. Cost in €. Significance levels: **: 1%, *: 5%, †: 10%.*

We estimate the transportation choice model by maximizing the log-likelihood defined by Equation (1). The estimated coefficients, presented in Table 2, have the expected signs. Individuals value negatively the cost of the trip as well as its duration. The interactions between the trip duration and individual characteristics reveal that the sensitivity to trip duration is more heterogeneous across age than across income categories. Older individuals are more sensitive to trip duration. But sensitivities to trip duration are not so different for

individuals between 25 and 60 years old. Sensitivity to trip duration depends non-linearly on wealth: it increases until the 4^{th} quintile and then decreases for the highest quintile. However, the coefficients in the first four quintiles are not significantly different. It reveals that the top-wealth individuals are less sensitive to trip durations than lower-wealth categories.

The transportation mode dummies reveal significant differences in the stand-alone preferences for different transportation alternatives. We also find that driving a car or taking public transport at peak hours are preferred to using these modes at off-peak hours. The value of the nest parameter is high (0.79), indicating that leaving at peak and off-peak hours are subject to relatively independent shocks and thus constitute imperfect substitutes. Yet, the coefficient is lower than one, implying a slight correlation between the preference shocks within transportation modes. The value of the nest parameter also confirms the relevance of the nest to represent substitution patterns between different transportation modes and departure times.

The interactions between the off-peak hour dummy and the socio-professional categories reveal that white-collar workers and young students are less flexible than the other categories. The most flexible individuals are the blue-collar workers, students in higher education, and independent workers. We also find that families dislike traveling outside peak hours, indicating lower schedule flexibility. Finally, the public transport controls have the expected signs: the number of layovers and the overcrowding reduce the utility of public transport. The railway dummy is positive but not significant.

We test the sensitivity of our estimation results to alternative model assumptions. All the robustness checks and the results are presented and discussed in Appendix C.1. To account for the possible role of unobservables correlated with the trip's duration, we check that adding weather variables or a measurement of travel time reliability as controls do not affect our estimates. We also estimate models with random coefficients on the duration, trip cost, or the off-peak hour dummy. We consider a model where car depreciation is included in the trip's cost, and also check how sensitive the results are to the choice of a functional form for the duration. We also provide the estimates when we rely on different car trip duration predictions at off-peak hours. We explore a model with two different off-peak hour periods (off-peak hours early and off-peak hours late) and a model with a different nesting structure. Finally, we check that our estimates are not very sensitive to the choice set availability assumptions.

3.3 Values of travel time and substitution across modes and periods

With these parameters, we compute individuals' values of travel time (or opportunity cost of time) in €/hr. The value of travel time represents how much an individual should receive (in €) to compensate for the decrease in utility related to an increase in travel time by an hour. Formally the VOT for individual n is:

$$\text{VOT}_n = \frac{\beta_n^{\text{duration}}}{\alpha} \times \frac{1}{\text{duration}_n},$$

where α is the sensitivity to the trip monetary cost. Because we specify the utility as a function of the logarithm of the duration, the marginal utility of duration depends on the trip duration. We, therefore, calculate the values of travel times associated with the chosen transportation modes and departure periods.

Table 3 presents detailed information about the distribution of the value of time across individuals. We obtain an average value of travel time of €15.9/hr which is higher than the median value of only €10.3/hr. We observe substantial heterogeneity in how individuals value their time in transport, reflected by the extreme minimum and maximum opportunity costs of time (€0.44/hr and €389/hr). However, the maximal value is an outlier since the 99$^{\text{th}}$ percentile of the distribution is much more reasonable (€81/hr). The mean value of travel time is in line with a recent study by Buchholz et al. (2020) that estimates an average value of time of $13.5/hr on a sample of cab riders in Prague. Our results are consistent with Parry and Small (2009) who estimate the mean valuation of travel time to be close to half the average hourly wage in London and Washington D.C. Our mean value represents 67% of the mean wage in 2012 in the Paris metropolitan area (€23.9/hr).[9] This is close to the ratio found by Goldszmidt et al. (2020) (75%) using natural field experiments on 13 U.S. cities. Our mean value of travel time is also consistent with Kilani et al. (2012), who estimate an average of €17/hr for a working father in Paris. Indeed, our estimate is for the whole population, and we expect working fathers to have higher opportunity costs of travel time than average. We show in Figure 6 of Appendix C.2 the distribution of VOT as function of age and income.

[9]Source for the average hourly wage in Paris: https://www.lemonde.fr/les-decodeurs/article/2016/11/28/en-ile-de-france-le-salaire-horaire-depasse-de-41-celui-des-autres-regions_5039717_4355770.html.

Table 3: Distribution of the values of travel time.

Min	p1%	Mean	Median	p99%	Max
0.44	1.34	15.9	10.3	81.1	389

Notes: in €/hr.

To better understand the substitution across departure periods for driving, we compute the own and cross elasticities to duration. We also calculate the own and cross elasticities to the car trip cost to put the values in perspective. Appendix C.2 gives the main statistics of their distributions. Results show large heterogeneity across individuals and lower elasticites at peak hour on average.

4 Estimation of the road traffic congestion technologies

4.1 Data and sample selection

We split the Paris area into five zones: the city center, the ring roads, the close suburb, the far suburb, and the main highways that connect the city center to the suburb. We estimate the congestion technology for three areas: the city center, ring roads, and highways. Because of data limitations, we cannot estimate the congestion technology for the suburbs. However, we still allow for adjustment of the equilibrium speeds in the close and far suburbs by assuming the same congestion technology as in the city center. To estimate the three road congestion technologies, we rely on hourly data on traffic conditions from road traffic sensors for 2016 and 2017. We provide more information about the data in Appendix C.3.1.

The traffic sensors typically record four variables: the traffic flow (in vehicles per hour), the traffic density (in vehicles per kilometer), the occupancy rate, i.e., the percentage of time during which the sensor detects a car (in percentage per hour), and the speed (in km/hr). The traffic flow, traffic density, and speed are related through the fundamental equation of traffic flow:

$$\text{traffic flow} = \text{speed} \times \text{traffic density}.$$

And the traffic density and occupancy rate are related through:

$$\text{traffic density} = \frac{\text{occupancy rate}}{\text{mean effective car length}} \times \text{no. lanes}.$$

The mean effective car length represents the length of the car plus the space between two vehicles. The data on the highways contain the four main traffic variables but the data from the city center and the ring roads do not record speeds. We thus use the fundamental equation above to estimate the speeds. We provide more details and explain how we construct

the final sample to estimate the congestion technology in Appendix C.3.1. Our final sample contains 1.9 million hourly observations for the ring roads recorded from 118 stations. We have 599 measurement stations recording 8 million observations for the city center.

Table 4: Road traffic conditions by area.

		Peak	Off-peak	All sample		
	Area	**Mean**	**Mean**	**Mean**	**Median**	**Std. dev.**
Speed	Highways	44.9	67	86	91	25.6
	City center	22.4	31.7	38.1	31.8	24.9
	Ring roads	30.4	57.9	56.3	61.1	21.3
Occupancy	Highways	23.4	14.1	7.92	5.84	7.67
	City center	17.2	6.17	6.04	3.75	7.52
	Ring roads	33.5	15.3	15.4	12.3	11.6

Note: Speed is in km/hr, and occupancy rate is in %. Averages at peak and off-peak hours are computed over workdays, excluding school and public holidays, and weighted by the average traffic flow of the traffic sensor. Peak hour is between 8:00 and 8:59 a.m., and off-peak hour is between 6:00 and 6:59 a.m.

Table 4 provides the summary statistics for the speeds and occupancy rates in the different areas. We observe significant heterogeneity across areas, suggesting that our partition is relevant. Speeds at peak and off-peak hours are significantly different, supporting our differentiation across periods. In addition to providing evidence of heterogeneity across areas, the traffic speeds and occupancy rates are highly variable; we leverage these variations to estimate flexible road congestion technologies.

4.2 Estimates of the congestion technologies

We use the observations on speed and occupancy rate to estimate the congestion technologies f^a in each area a. We approximate them by Bernstein polynomials of degree seven and impose the constraint that the functions are weakly decreasing when estimating the coefficients of the polynomials $(c_0^a, ..., c_7^a)_{a=1,...,A}$.[10] The identification of the relationship between speed and traffic comes from the local variation in traffic conditions in the data. We exploit several dimensions of variation between observations in the traffic data. First, we expect different hours to have heterogeneous traffic levels: traffic should be heavier at peak hours in the morning and evening. Second, traffic conditions are presumably variable across weekdays, weekends, public holidays, and school holidays. In addition, we observe data for different roads within an area that may also have different traffic conditions. We provide the fits of the models for each area in Appendix C.3.2.

[10]The constraints are: $c_l^a \geq 0 \quad \forall l$ and $c_{l+1}^a \leq c_l^a \quad \forall l = 0, ..., L-1$.

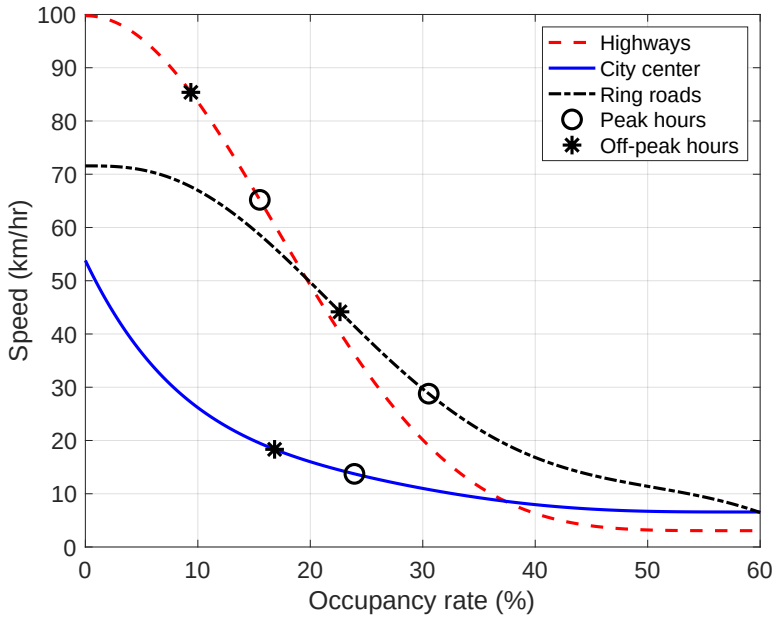

Figure 1: Estimated congestion technologies and initial traffic conditions.
Note: Initial conditions are average speeds at peak and off-peak hours from TomTom predicted durations.

As Figure 1 shows, the estimated values of the maximal speeds are very much in line with the maximum speed limits in each area. We estimate it to be 99.8 km/hr for highways compared to speed limits that vary between 90 and 130 km/hr depending on the road and the location. The speed limit is typically 70 km/hr on the ring roads, very close to our estimate of 71.6 km/hr. Lastly, the speed limit was usually between 30 and 50 km/hr in the city center at that period, but individuals may not always comply with the speed limit. Therefore, our estimate of 53.8 km/hr shows high consistency again. Our congestion technologies show heterogeneity across the city areas. We have a high speed for low occupancy rates on highways, but it becomes slower than any other area for high congestion levels. This can be explained by the role of interchanges, entries, and exits on highways, which may slow down driving speeds quickly when the traffic increases. This implies a critical difference of 20.2 km/hr in speeds between peak and off-peak hours. The congestion curve for ring roads remains flat initially: the slope remains higher than -0.3 until an occupancy rate of 4.2%. In contrast, the speed in the city center displays a convex relation, with speeds decreasing faster for lower occupancy rates than for larger ones. Overall, our estimates reject the assumption of a single, city-wide, congestion technology and show that the congestion technologies do not follow simple functional forms.

Our estimates could suffer from an endogeneity bias if the same unobserved shocks affect

the occupancy rate and speed. We do two sensitivity analyses adding additional controls to decrease the propensity to have common unobserved shocks. First, we exclude observations with extreme weather. Second, we estimate congestion technologies that are allowed to be heterogeneous across traffic measurement stations, hours of the day, days of the week, or dates. We discuss the underlying assumptions behind these robustness checks and their results in Figures 9 and 10 in Appendix C.3.2. Our benchmark estimated congestion technologies are not systematically higher or lower when we estimate different specifications or use restricted samples, suggesting that we do not have biases.

4.3 Mapping between individual decisions and initial traffic conditions

Our transportation mode choice model predicts the individual probabilities of driving at peak and off-peak hours given car trip durations. We have considered that car trips are fixed and observed for the estimation. In our equilibrium model, however, car trip durations depend on the speeds and distances in each area. More specifically, the car trip duration for individual n at period t is given by:

$$\text{duration}_{nt} = \sum_{a=1}^{A} \frac{k_n^a}{v_t^a} \times \varepsilon_{nt}.$$

k_n^a represents individual n's distance in area a and v_t^a is the speed. Note that if the itinerary of an individual does not include an area, distance is set to 0. ε_{nt} represents an individual and period-specific multiplicative speed shock, which constitutes another structural parameter of our model. It captures individual-specific unobserved trip characteristics that make an individual average speed lower or higher than the average. We assume these shocks are exogenous to the traffic conditions and hold them constant when we simulate new traffic equilibria. We take the logarithm of the previous equation and estimate the inverse of the initial speeds $\frac{1}{v_t^a}$ and recover the individual speed shocks $\tilde{\epsilon}_{nt}$ (they are the residuals). We estimate the speeds for each period separately using trip durations from TomTom and trip distances using the non-linear least squares method:

$$\log(\text{duration}_{nt}) = \log\left(\sum_{a=1}^{A} \frac{k_n^a}{v_t^a}\right) + \tilde{\varepsilon}_{nt}.$$

The estimated speeds are provided in Table 5. Speeds are always higher at off-peak hours than peak hours. They are also much higher on the highways, then on the ring roads and far suburb and finally in the city center and the close suburb. These estimated speeds also reveal that the difference in speeds between peak and off-peak hours is very similar for the city center and the close suburb, which is consistent with our assumption that these two

areas share the same congestion technology.

Table 5: Estimated average speeds from TomTom data.

	Peak hours		Off-peak hours	
Area	**Average speed**	**Std. errors**	**Average speed**	**Std. errors**
Highways	65	0.849	85.8	0.975
City center	13.8	0.137	18.3	0.158
Ring roads	27.7	0.464	46.5	0.716
Close suburb	15.9	0.102	20.2	0.111
Far suburb	25.5	0.131	29.2	0.132

Note: Speeds in km/hr. Standard errors are computed using the delta-method from the estimates of the inverse of speeds.

With these estimated initial speeds, we then back out the initial occupancy rates by inverting the congestion technologies:

$$\tau_t^a = \left(f^a\right)^{-1}(v_t^a).$$

τ_t^a is unique since f^a is decreasing in speed. Finally, we consider a mapping between the number of individuals driving and the occupancy rate in each area and period. We assume an affine relation between the occupancy rate, which is the argument of the speed function, and the total number of kilometers driven. We choose to consider the number of kilometers driven because the traffic depends on how many individuals decide to drive and how long they drive. Formally, we consider:

$$\tau_t^a = \phi_t^a \times K_t^a + \gamma_t^a.$$

ϕ_t^a is a scale parameter representing the inverse of the size of the area while γ_t^a reflects irreducible traffic or traffic that is not due to households (buses, delivery trucks, etc...). We can only identify two parameters per area because we observe individual choices and speeds for only two periods. We therefore impose that $\phi_t^a = \phi^a$ and $\gamma_t^a = \gamma^a$. Instead, we could impose some restrictions across areas and let the parameters vary with the period. But given that the areas have very different sizes and may be subject to different levels of irreducible traffic, our assumption seems more appropriate.

Using the initial occupancy rates and the predicted number of individuals in each area given the initial speeds, we solve for ϕ^a and γ^a such that:

$$\tau_t^a = \phi^a \times K_t^a + \gamma^a.$$

With two linear equations and two unknowns we can find a unique pair of parameters for each area. We further impose that the shares of irreducible traffic are between 0 and 60%

and use the constrained least-squares method that minimizes the sum of square deviations from the equations above. The calibrated parameters are presented in Table 6. We obtain a rather large irreducible share of traffic in the close suburbs (21.6%) and the city center (13.3%) while we estimate no irreducible traffic for highways and the ring roads. We provide the comparison between observed and predicted transportation mode shares and speeds in Appendix C.3.3 and obtain a good fit of the model.

Table 6: Calibrated parameters of the mapping between occupancy rates and driven distances.

Area	**Scale parameter** ($\phi^a \times 10{,}000$)	**Irreducible traffic** (γ^a)	**% irreducible traffic** ($\gamma^a / \tau^a_{\text{peak}} \times 100$)
Highways	0.024	0	0
City center	0.373	3.18	13.3
Ring roads	0.372	0	0
Close suburb	0.115	4.37	21.6
Far suburb	0.011	6	57.3

Notes: The share of irreducible traffic is in % of peak hour occupancy rates.

4.4 Check of the equilibrium uniqueness

We now apply the method developed in Section 2.3 to verify that our algorithm is a contraction. Given the estimated model parameters, we check that the model has a unique equilibrium. We compute the Lipschitz coefficients for values of the algorithm tuning parameter κ between 0 and 0.99. We solve for these coefficients at the equilibrium speeds without policy and under the different policy environments that we consider in section 5. We compute:

$$\max_{a \in A} \max_{t \in T} \max_{a' \in A} \max_{t' \in T} \left| \frac{\partial g_t^a(\mathbf{v}^*, \kappa)}{\partial v_{t'}^{a'}} \right|,$$

where $\mathbf{v}^*$ denotes the vector of equilibrium speeds. Panel (a) of Figure 2 shows several interesting insights. When κ is very low, i.e. when we put a low weight on the previous speed value, the algorithm is not a contraction. We also find that the policies do not modify the Lipschitz coefficients of the algorithm. Finally, the variable toll policy requires the highest κ to have a contraction. We also check for which values of the tuning parameters our algorithm is a contraction in the entire set of possible speed values in their interval $[\underline{\mathbf{v}}, \overline{\mathbf{v}}]$. This time we calculate:

$$\max_{a \in 1,\ldots,A} \max_{t \in 1,\ldots,T} \max_{a' \in 1,\ldots,A} \max_{t' \in 1,\ldots,T} \max_{\mathbf{v} \in [\underline{\mathbf{v}}, \overline{\mathbf{v}}]} \left| \frac{\partial g_t^a(\mathbf{v}, \kappa)}{\partial v_{t'}^{a'}} \right|.$$

Panel (b) of Figure 2 shows that there are values of $\kappa < 1$ for which the function is a contraction on the entire space of the speeds. From $\kappa = 0.53$, the algorithm is a contraction. This time, we find that the no-policy environment is associated with the smallest set of κ that ensures our algorithm is a contraction. The lowest value of κ that corresponds to the

lowest Lipschitz coefficients under the different policy environments is thus 0.65. We use this value to solve the equilibrium speeds in the different counterfactual simulations.

Figure 2: Lipschitz coefficients at the equilibrium speed and for any speed.

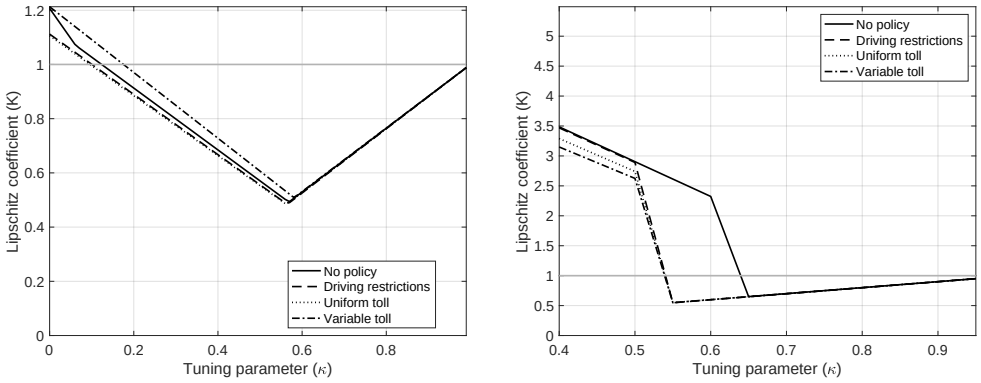

(a) At the equilibrium speeds. (b) In the space of all possible speeds.

We show in Appendix C.4 that the number of iterations and the computation time needed to solve the model for different values of κ in the no policy environment. We can see that they increase exponentially with the tuning parameter. We obtain the highest speed for $\kappa = 0.5$. However, the value we choose, $\kappa = 0.65$, multiplies the convergence time by only around 1.5.

4.5 Value of driving and marginal costs of congestion

First, we measure the value of driving at peak hours at the initial equilibrium speeds. If individuals could not take their cars at peak hours, they incur a surplus loss of €2.56 million, corresponding to 79 cents per trip for a potential driver.[11] Second, we measure the value of driving at peak hours under maximum speeds, given the irreducible portions of traffic in each area. The improvements lead to a total surplus increase of €6.12 million, corresponding to €1.90 per potential driver. The value of driving at peak hours at maximum speeds is 2.4 times that of driving at initial speeds, highlighting the detrimental effect of congestion in the Paris metropolitan area. Congestion generates a total increase in travel time of 396 thousand hours, equivalent to an average additional 7.4 minutes per driver, increasing the average trip duration by 23.6%.

We define the marginal costs of congestion for an area, at a given period, as the total surplus losses associated with one additional kilometer driven or an extra driver in that area. For the case of the extra driver, we add the average number of kilometers driven by

[11] A potential driver is an individual who owns a car.

an individual in that area. Adding one kilometer or a car marginally affects the area speed, which in turn increases car trip durations by a small amount for everyone driving in that area. Finally, we calculate the surplus variation from these marginal changes at the individual level. The society marginal cost thus corresponds to the sum of all surplus variations.

Table 7 shows area-specific marginal costs for an additional kilometer between 2 and 53 cents. The highways and the far suburb have the lowest marginal costs. This is a consequence of area size; one additional kilometer does not significantly impact the traffic density. Globally, the costs associated with an additional driver are between 34 cents and €2.1. The initial marginal costs are higher at peak hours than at off-peak hours. But the difference between periods is highly heterogeneous across areas. The differences are small in the city center and the suburbs. However, the highways exhibit a much larger difference; the marginal cost of congestion per driver at peak hours is 2.7 times larger than at off-peak hours. The marginal costs depend on two key model parameters. First, the slopes of the congestion technologies are higher at peak hours than during off-peak hours in all areas. The second key parameters are the marginal valuations of travel time. Since our utility specification is logarithmic in the duration, and trip durations are higher at peak hours than at off-peak hours, the values of travel time are higher at peak hours. Finally, we also compute a marginal cost of congestion where we add an individual driving with the average itinerary (i.e., distance traveled in each area) among individuals owning a car. The average costs are €2.97 at peak hours and €1.87 at off-peak hours.

The most appropriate way to compare our results to results in the literature is to use our estimates of the marginal costs of congestion per kilometer. Making such a comparison puts our congestion values close to Couture et al., 2018 (3.6 cents of $ for several U.S. cities), Akbar and Duranton, 2017 ($10 cents for Bogota), and Yang et al., 2020 (3 yuan or approximately €36 cents for Beijing).[12]

Table 7: Estimated initial marginal costs of congestion by area.

	One kilometer (in cents)		**One average driver (in €)**	
Area	**Peak**	**Off-peak**	**Peak**	**Off-peak**
Highways	7.63	1.7	1.14	0.415
City center	53.2	42	1.58	1.26
Ring roads	44.8	25	2.09	1.19
Close suburb	45.3	36	1.29	1.04
Far suburb	8.22	4.3	0.582	0.339
Average			2.97	1.87

Note: "Average" is the marginal cost for the average driver's itinerary.

[12]We use the average 2014 CNY-EUR exchange rate from https://www.exchangerates.org.uk/CNY-EUR-spot-exchange-rates-history-2014.html.

5 Quantifying the welfare consequences of the regulations

Using the transportation choice model and estimated road technologies, we study the welfare effects of three policies: (1) driving restriction banning a fraction of cars randomly, (2) a uniform toll, and (3) a variable toll linear in the trip's distance. We only focus on policies applicable at peak hours so that driving at off-peak hours is never constrained. Our model predicts individual probabilities of choosing each transportation mode and the equilibrium driving speeds at peak and off-peak hours in the five areas. Thus, we do not predict counterfactual choices but individual choice probabilities, which we use to compute the expected number of individuals choosing each transportation mode and departure period.

The estimated effects correspond to one trip per person for the entire population of commuters in the Paris area. There are, on average, 253 working days annually and two commuting trips per day, so we should roughly multiply the costs by 500 to convert them into annual terms. Next, we measure the policies' impacts on consumer surplus, tax revenue, and emissions. We define two aggregate welfare measures. The first is the sum of the change in consumer surplus and tax revenues, and the second also incorporates the benefits from avoided emissions valued at standard levels. In Appendix D.1, we provide additional details on how these welfare measures are defined, as well as the decomposition we use to separate policy effect into a pure policy effect at constant speeds and an effect from speed changes.

To study the importance of accounting for speed adjustments to accurately predict the transportation policies' effects, we compare the outcomes predicted by our model against those obtained under a simpler model with constant speeds. The comparison, provided in Appendix D.2, illustrates the importance of considering the policies' effects on congestion levels and driving rates, as they influence substitution patterns between transportation modes and departure periods.

5.1 Analysis of different policy levels

To properly compare the three policies at different stringency levels, we rely on the percentage reduction of the total number of kilometers driven at peak hours. Figure 3 presents the surplus losses, tax revenues, and welfare (excluding emissions) changes associated with the three policies. The impact of the driving restriction on consumer surplus increases linearly with the stringency level. The uniform toll has a concave relationship, while the variable toll has a convex shape. This indicates large differences in how individuals react to a policy's stringency level. Increasing the price of a uniform toll has a lower marginal impact on individuals, while

the effect increases in the case of a variable toll. The variable toll achieves the lowest surplus losses across all stringency levels by targeting high-distance drivers. Panel (b) shows that under both types of tolls, we obtain Laffer curves, and the total tax revenue decreases at high toll values. We also note that the uniform toll is better at generating revenue than the variable toll for almost all stringency levels, except for the highest. Nonetheless, the variable toll remains the most efficient policy across stringency levels after redistributing the tax revenue. As Panel (c) shows, the two types of tolls have positive welfare impacts for moderate stringency levels after tax-revenue redistribution. Uniform (respectively variable) tolls generate welfare gains for reductions in the driving distance below 35% (respectively 50%). These are policies with a uniform toll below €2.7 or a variable toll of €0.15/km. The optimal uniform and variable tolls maximizing total welfare are €1.4 and 8 cents/km, respectively. The optimal variable toll reduces traffic much more than the uniform toll (28.2% against 18.2%). The welfare difference is however relatively small: the variable toll leads to €33,000 higher gains than under the uniform toll.

Figure 3: Change in individual surplus, tax revenue and welfare.

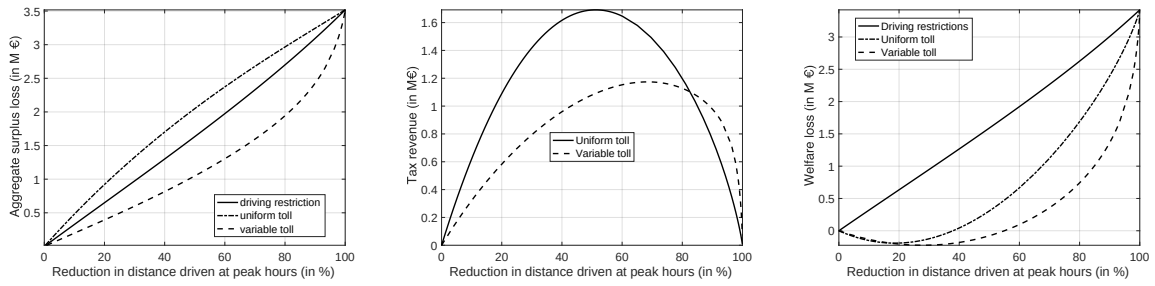

(a) Surplus losses. (b) Tax revenues. (c) Welfare losses (W_2).

Figure 4 presents the aggregate surplus losses using distributional weights (the inverse of wealth), the range of surplus losses (difference between maximum and minimum surplus losses), and the difference in surplus variation between the top and bottom 10% of the income distribution. Using distributional weights does not affect the policy ranking nor the aggregate surplus loss magnitudes, as seen in Panel (a). However, Panel (b) highlights the main disadvantage of the variable toll and its distributional impacts: while the uniform toll and driving restrictions generate almost the same surplus difference, it is two times larger under the variable toll. This result highlights how policymakers' secondary objectives might affect the choice of a policy instrument, as the variable toll generates the highest aggregate surplus but also the largest inequalities.

Figure 4: Change in distributional outcomes.

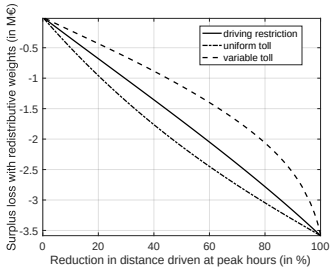

(a) Surplus losses with distributional weights.

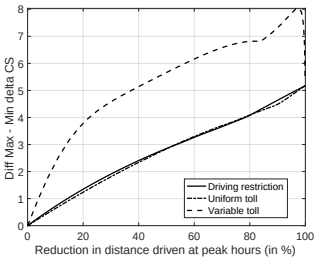

(b) Surplus loss range.

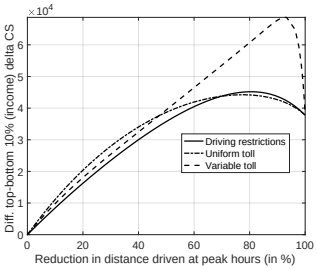

(c) Difference in surplus loss between the top and bottom 10% of the income distribution.

Figure 5 presents the costs associated with the different policy stringency levels. Panels (a) and (b) show that the three policies have similar impacts on total emissions of equivalent NO_X and CO_2, with the uniform the most effective policy and the driving restriction the least effective. The differences across policies mainly come from differences in substitution for driving at off-peak hours. The policies also discourage different individuals from driving, affecting the composition of drivers and the total emissions. The variable toll generates the most extensive substitution for driving at off-peak hours, limiting its impact on emissions. In contrast, the uniform toll discourages short trips, which usually have better alternatives outside cars. Panel (c) provides the average costs of the regulations. The average costs of reducing emissions increase with the policy stringency under the two types of tolls: linearly for the uniform toll, while the relationship is convex under a variable toll. In sharp contrast, the cost function decreases with the policy stringency under driving restrictions, reflecting that the welfare losses increase more slowly than the decrease in emissions. Price instruments can have negative costs for low stringency levels, consistent with the net benefit we obtain after the tax redistribution. We can find a more extensive set of policies with a negative cost of reducing emissions under the variable toll despite being less effective at decreasing emissions.

Figure 5: Average cost of reducing emissions of local pollutants.

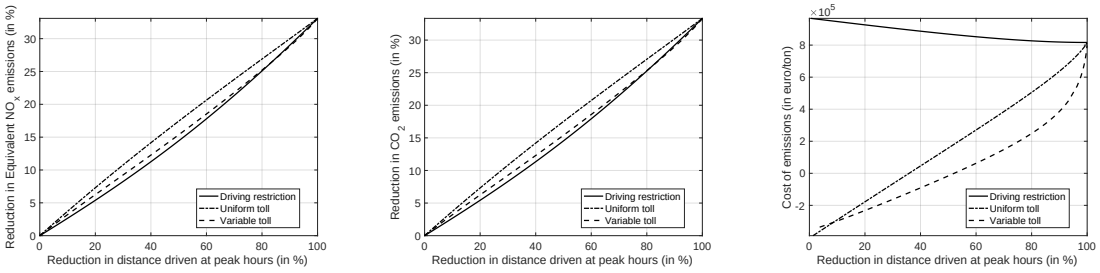

(a) Eq-NO_X emissions. (b) CO_2 emissions. (c) Cost in €/ton eq-NO_X.

5.2 Comparison across policies at a benchmark level

To further analyze the effects of the previous policy instruments, we set a benchmark policy stringency level. We calibrate the road tolls to achieve the same traffic reduction at peak hours as a driving restriction that bans individuals from driving with a probability of one-half. This policy mimics one based on whether the last digit of the license plate is odd or even. The equivalent uniform toll is €2.69 while the variable toll is 10 cents/km. All three regulations reduce the number of kilometers driven by 34% at peak hours.[13] With two trips per day, the uniform toll implies a total cost of €5.4 per day, close to the London congestion charge before 2007.[14] The variable toll of €0.10/km implies an average cost of €1.43, lower than the uniform toll. The maximum variable toll reaches €14.1 for the longest distance.

Impacts on consumer surplus Table 8 presents the policies' impacts on consumer surplus. The ranking of policies by surplus losses and welfare changes follows the results from the previous section, and the policy costs are between €0.7 million and €1.5 million. As we saw in the previous section, toll revenues are huge and cover 102% and 128% of the total surplus loss for the uniform and variable tolls, respectively. If we redistribute the entire tax revenue, the tolls generate benefits between €27,000 and €181,000. As long as the shadow cost of public funds is below 75%, both tolls outperform the driving restriction policy, which is very likely to be the case in reality. To better understand the role of the changes in speeds induced by the different policies, we decompose the total variation in consumer surplus into two terms: the variation in consumer surplus due to the policies keeping the speeds constant and the changes in surplus induced by the modification of the equilibrium speeds. While

[13] An alternative benchmark would match the total distance driven at peak and off-peak hours across policies. We would obtain slightly lower calibrated tolls.

[14] The London toll implemented in 2003 was initially £5/day and increased to £8 in 2005, £10 in 2011, £11.5 in 2011, and £15 in 2020.

speed improvements always create welfare gains, they are insufficient to offset the policy welfare costs since they only cover between 13% and 34% of the aggregate surplus losses.

Across policies, there is a constant share of individuals with no change in their surplus. These are individuals without a car who are not affected by the regulations. No individual has surplus gains under a uniform toll. The driving restriction induces a tiny portion of individuals to have positive surplus changes (around 3,000 individuals out of 4.03 million). In contrast, 18.9% of the population is better off under a variable toll. The winners are those with short trips and high valuations of time, which continue to drive at peak hours since their toll is low. Among the winners, the average toll is €0.29 versus an average toll of €1.44 for all individuals holding a car.

Table 8: Consumer surplus variation under the benchmark policies.

	Driving restriction	**Uniform toll**	**Variable toll**
Total ΔCS (M€)	-1.11	-1.49	-0.69
ΔCS, constant speed (M€)	-1.28	-1.69	-0.93
ΔCS from speed (M€)	0.164	0.199	0.24
Total ΔwCS (M€)	-1.16	-1.55	-0.752
Tax revenue (M€)	0	1.52	0.871
ΔW_1 = ΔCS + tax revenue (M€)	-1.11	0.027	0.181
ΔW_2 = ΔCS + tax rev. - ΔE (M€)	-1.09	0.064	0.212
% ΔCS = 0	20.3	20.3	20.3
% ΔCS > 0	0.075	0	18.9
% ΔCS < 0	79.7	79.7	60.8

Note: "ΔE" are changes in emissions valued at standard levels.

Winners and losers We now characterize winners and losers by analyzing the surplus changes by demographic groups based on age, wealth, socio-professional activity, family size, and trip distance. We consider the surplus changes without tax revenue redistribution. Table 9 shows that the ranking of policies is identical for all subgroups of individuals except for the highest distance quantile, for which the mean surplus decreases the most under the variable toll. The category of individuals under 18, students in kindergarten, elementary, middle and high school, and individuals with trips less than 11.5 km are the least affected under the variable toll. These subgroups lose less than €10 cents. This is due to the short distance of their trips, implying gains from improved speeds at peak hours and low toll costs. In addition, the two lowest distance quintiles have a positive surplus variation; while all the other groups are associated with losses. Across all policies, the most affected individuals are those between 35 and 60 years old, the two lowest wealth quintiles, those with a family, and the longest distance commuters. Among employed individuals, white-collar workers are the most affected by the policies. Our transportation choice model indeed suggests that blue-collar workers have the lowest disutility from driving outside peak hours, reflecting higher flexibility in their

schedules. Except for individuals with short commutes, there is little heterogeneity in the policies' effects across trip distance for the driving restriction and the uniform toll, while the heterogeneity of the policies' effects according to trip distance is more pronounced for the variable toll.

Table 9: Average surplus variation by demographic group.

	Driving restriction	**Uniform toll**	**Variable toll**
Age $<$ 18	-0.228	-0.303	-0.057
Age $\in$ [18-25[	-0.195	-0.269	-0.148
Age $\in$ [25-35[	-0.272	-0.366	-0.184
Age $\in$ [35-45[	-0.322	-0.43	-0.237
Age $\in$ [45-60[	-0.327	-0.437	-0.238
Age $\geq$ 60	-0.306	-0.403	-0.178
Wealth $\leq$ 110,000	-0.303	-0.4	-0.207
Wealth $\in$]110,000-152,000]	-0.32	-0.423	-0.213
Wealth $\in$]152,000-205,000]	-0.299	-0.397	-0.188
Wealth $\in$]205,000-283,000]	-0.252	-0.341	-0.141
Wealth $\geq$ 283,000	-0.208	-0.288	-0.106
Independent	-0.298	-0.419	-0.241
White collar	-0.331	-0.427	-0.223
Blue collar	-0.283	-0.394	-0.213
Education $\leq$ high school	-0.233	-0.309	-0.059
Education $>$ high school	-0.128	-0.185	-0.113
Family	-0.29	-0.388	-0.18
Single	-0.205	-0.276	-0.126
Distance $\leq$ 2.05 km	-0.174	-0.245	0.02
Distance $\in$]2.05, 5.4] km	-0.284	-0.384	0.002
Distance $\in$]5.4, 11.5] km	-0.303	-0.404	-0.087
Distance $\in$]11.5, 21.4] km	-0.289	-0.387	-0.231
Distance $>$ 21.4 km	-0.331	-0.43	-0.56
Average	-0.276	-0.370	-0.171

Note: in €/trip.

Environmental impacts The results in Table 10 below show the differences between policy instruments' efficiency in reducing carbon and local pollutant emissions. The three policies have roughly the same impact: they reduce carbon emissions by 300 to 380 tons of CO_2 emissions while the decreases in local pollutant emissions lie between 1.2 and 1.6 tons of equivalent NO_X emissions. As a robustness check, we measure the policy effects on emissions using our alternative estimates of car local pollutant emissions that depend on driving speeds (see Appendix B.2.2). We obtain slightly more emissions avoided, but the heterogeneity patterns across pollutants and policies remain identical. Overall, the speed improvements are responsible for a small share of the total decrease in emissions, representing at most 20.5% for HC emission changes and 11.6% for NO_X emissions.

Table 10: Changes in emissions under the different policies.

	Driving restriction	Uniform toll	Variable toll
Main emissions estimates			
ΔCO_2	-300	-383	-330
ΔNO_X	-0.379	-0.481	-0.432
ΔHC	-0.104	-0.134	-0.112
ΔPM	-0.052	-0.068	-0.057
ΔEq. NO_X	-1.24	-1.59	-1.37
Alternative emissions estimates (Copert)			
ΔNO_X	-1.05	-1.3	-1.08
ΔHC	-0.071	-0.088	-0.064
ΔPM	-0.048	-0.06	-0.051
ΔEq. NO_X	-1.84	-2.28	-1.92
Relative importance of speed changes (Copert)			
NO_X	11.6	9.9	10.3
HC	19.7	18.8	20.5
PM	8.12	6.88	7.38
Eq. NO_X	10.2	8.66	9.01

Note: Δ emissions in tons. "Eq. NO_X" aggregates the local pollutants into equivalent NO_X emissions. Relative importance in %.

Average costs of regulations We calculate the average costs of reducing carbon and local pollutant emissions separately. The results, presented in Table 11, show that the costs of regulations are around 240 times lower for a ton of CO_2 emissions than for a ton of equivalent NO_X emissions. The report from the DG MOVE (2014) suggests that the value of a ton of CO_2 is 326 times lower than that for a ton of NO_X; thus, our emissions costs are in line with the relative value for NO_X and CO_2 emissions. However, the estimated costs of reducing emissions are at least 40 times higher than the social values (the report of the DG MOVE (2014) recommends €13,000/ton of NO_X and €50/ton of CO_2). However, during a pollution peak, we expect the social cost of emissions to be much higher than the long-term values of emissions savings. To our knowledge, there is no recommendation for the value of emissions under these circumstances.

Table 11: Average costs of regulation for the different policies.

		Driving restriction	Uniform toll	Variable toll
w/o redistribution	ΔCO_2	3,720	3,893	2,094
	$\Delta EqNO_X$	897,728	935,863	502,556
with redistribution	ΔCO_2	3,720	-72	-549
	$\Delta EqNO_X$	897,728	-17,192	-131,690

Note: in €/ton.

In Appendix D.3, we analyze more outcomes: the substitution patterns across transportation modes, travel time variations, and the marginal costs of congestion under the different policies.

Robustness checks We focus on peak-hour policies for two reasons. First, congestion is most severe at peak hours, leading to high pollution levels and more time spent in traffic. The second reason is technical: in our sample, we observe individuals without alternatives to driving, so they cannot comply with driving restrictions applicable all day. To analyze such all-day driving restrictions, we make assumptions regarding non-compliance costs and provide the results in Appendix D.6.1. The ranking across policies remains the same, but the regulations are costlier for individuals, as inter-temporal substitution is no longer possible.

Our analysis holds the quality of public transport constant. In Appendix D.6.2, we check the sensitivity of the results to changes in the overcrowding levels in public transport. We consider the benchmark variable toll and two scenarios where overcrowding levels increase by 15% and 30%. These assumptions are rather extreme since public transport usage at peak hours increases by 11% in our benchmark. We find minimal changes in the transportation mode shares and equilibrium speeds. The total surplus loss would be 9% and 18% higher in the two scenarios, highlighting the small role of public transport overcrowding.

In our benchmark model, we do not consider the role of travel time reliability and how it could be affected by hypothetical policies. In Appendix D.6.3, we use a transportation choice model specification that includes travel time reliability and analyze how the welfare results change when we improve the driving time reliability level at peak hours. A 46.5% decrease in travel time reliability at peak hours increases car usage by less than 1% at peak hours, suggesting that reliability plays a limited role in individual transportation decisions. Furthermore, the improvement reduces the aggregate surplus losses by 23%.

6 Mitigating the surplus losses

6.1 Welfare-maximizing personalized tolls

To put our welfare measures in perspective, we compare surplus losses obtained under the variable toll to a first-best benchmark. We define first-best as a situation where the social planner sets personalized road tolls to maximize a welfare measure subject to a traffic-level constraint. Formally, we solve the following social planner problem:

$$\begin{aligned} & \max_{\{\mathbf{v},\mathbf{p}\}} W(\mathbf{v}, p_n) \\ \text{such that} \quad & \textstyle\sum_{n=1}^{N} \omega_n k_n s_{nt}(\mathbf{v}, p_n) = \bar{K}_t \quad \text{for } t = \text{peak hours} \\ & v_t^a = f^a\left(K_t^a(\mathbf{v}, \mathbf{p})\right) \quad \forall a = 1, ..., A, \qquad t = \{\text{peak, off-peak}\} \end{aligned}$$

We consider three different objective functions to maximize: aggregate consumer surplus, the sum of consumer surplus and tax revenue (W_1), and the sum of consumer surplus and

tax revenue minus the cost of emissions (W_2). The regulator is subject to two types of constraints. First, the total traffic (represented by the total number of kilometers driven at peak hours) should meet the objective, $\bar{K}_t$. Second, the social planner considers the road congestion technologies that determine the equilibrium speeds in each area. We additionally put some bounds on the toll values: tolls must be positive and below or equal €50.[15] Here, we compare policies that achieve the benchmark traffic reduction (34%). Still, we can solve for welfare-maximizing personalized tolls associated with any traffic level to calculate the optimal traffic reduction and the set of personalized tolls to achieve it (see Figure 15 in Appendix D.4).

Table 13 shows that under all objectives, the aggregate consumer surplus decreases, indicating that the reduction in traffic has a cost in terms of surplus. Maximizing consumer surplus leads to no tax revenue. The reason is that the distribution of tolls has almost a bi-modal distribution (see Table 12): 61% of drivers are subject to zero tolls, while 39% of them pay tolls greater than €26.6. Such personalized tolls thus act as targeted driving restrictions and reduce the surplus losses by a factor of 6.3. When we include the tax revenue in the welfare outcome, we obtain positive effects of the personalized tolls, and they multiply the gains by between 1.6 and 1.7. The personalized tolls are much more moderate since they lie between zero and €11.6. Furthermore, less than 1% of drivers do not pay any toll. This is due to the inclusion of tax revenue which increases with the toll value until reasonable values. Due to the relatively low social cost of emissions, including them in the objective of the social planner leads to only marginal changes in welfare impacts and the distribution of personalized tolls, as can be seen in Table 12.

While welfare maximizing tolls lead to a larger share of the population with a lower surplus (71.1% of the people versus 60.8% under the variable toll), we see that the losers are less hurt than under the variable toll (the minimal surplus change is -€3.14 and -€3.07 against -€4.07 under the variable toll). In contrast, the maximal gain is also higher under welfare-maximizing personalized tolls.

Table 12: Distribution of the personalized tolls.

	Min	**p25%**	**Median**	**p75%**	**Max**
Max. CS	0	0	0	37.7	50
Max. W_1	0	0.702	1.82	3.46	10.9
Max. W_2	0.003	0.708	1.85	3.54	11.6

[15] We could consider alternative objectives for the social planner, such as sum of consumer surplus with redistributive weights or assign different weights to the components of W_2.

Table 13: Welfare effects of personalized tolls.

	Variable toll	**Personalized tolls**		
		Max. CS	**Max. W_1**	**Max. W_2**
Total ΔCS (M€)	-0.691	-0.11	-0.778	-0.775
ΔCS, constant speed	-0.931	-0.588	-1.12	-1.12
ΔCS from speed	0.24	0.478	0.345	0.349
Total ΔwCS (M€)	-0.752	-0.18	-0.796	-0.792
Tax revenue (M€)	0.872	0	1.08	1.08
ΔW_1 = ΔCS + Tax revenue (M€)	0.181	-0.11	0.307	0.306
ΔW_2 = ΔCS + tax rev. - ΔE (M€)	0.212	-0.065	0.346	0.347
Δ CO_2 (ton)	-330	-469	-420	-428
Δ eqNO_X (ton)	-1.37	-1.95	-1.74	-1.78
% ΔCS > 0	18.9	48.9	8.66	8.63
% ΔCS < 0	60.8	30.9	71.1	71.1
Min ΔCS (€)	-4.07	-4.14	-3.14	-3.07
Max ΔCS (€)	0.766	2.49	1.35	1.37

Note: "ΔE" are changes in emissions valued at standard levels.

Since implementing personalized prices might be too difficult in practice, we investigate other flexible yet feasible road toll schemes. We measure the impacts of location-specific tolls (inside and outside of the city center) and tolls composed of a fixed part and a variable (kilometer-based) part in Appendix D.4. Table 14 below summarizes the welfare gains achieved by the different second-best tolls. The two-part toll, with a fixed fee and variable part, achieves 78% of the welfare gains obtained under the welfare-maximizing personalized tolls. The simple variable toll is relatively efficient since it generates 69% of the maximal welfare gains. The area-specific and uniform tolls have lower performances and generate 42% and 21% of the welfare gains under personalized tolls, respectively.

Table 14: Welfare effects of personalized tolls versus second-best instruments.

	ΔW_2 (M€)	$\%\Delta W_2$ w.r.t. personalized tolls
Personalized	0.306	100
Fixed and variable	0.24	78.4
Variable	0.212	69.2
Area-specific	0.127	41.5
Fixed	0.064	20.7

In Appendix D.5, we study an auction resembling Shanghai's vehicle license regulation (see Li, 2018). The policy leads to slightly larger tax revenues and greater emissions reduction. However, this policy generates larger surplus losses because by not buying a driving license, individuals commit to not driving, which is costly for individuals. In the end, this policy instrument decreases the total welfare.

6.2 Attribute-based driving restrictions

Low emission zone policies are widely used in Europe.[16] They impose driving restrictions based on combinations of fuel type and vintage to remove the most pollutant cars from the roads. Attribute-based policies are thus more cost-efficient at reducing emissions but generate greater distributional consequences than simple driving restrictions. We study the trade-off faced by policymakers by comparing the standard driving restrictions against two attribute-based policies: one banning all vehicles below a particular vintage and one banning diesel cars with a certain probability. While individuals are likely to change their cars in response to such policy, as shown by Barahona et al. (2020), we abstract from any effect on the fleet's composition.

As before, we calibrate the policies to reach the same traffic reduction as under the regular driving restriction. Since car vintage is a discrete variable, we cannot exactly match the expected number of kilometers at peak hours with this parameter only. We use the strictest vintage and assume that individuals are subject to the policy with a certain probability. For the diesel-based restriction, we assume all diesel cars have a probability of being affected. These technical assumptions can be interpreted as the frequency at which the policy is implemented. The calibrated are as follows: the vintage selected is 2006, above the average car vintage of 2004, and the policy should be applied 90% of the time. This regulation restricts 50.8% of the population. The diesel-based restriction should be applied 72% of the time and affects 47.6% of the people.

As Table 15 suggests, the vintage-based policy is slightly more costly for individuals, generating €1.19 million of surplus losses versus €1.11 million for the standard driving restriction. In contrast, the diesel-based restriction causes lower surplus losses (€1.03 million). Under the vintage-based and diesel-based regulations, 28.9% and 32.2% of the population experience a surplus increase, highlighting the existence of distributional effects. Aggregate surplus losses measured using the redistributive weights are significantly higher for both attribute-based policies than for the standard driving restriction, pointing out that they hurt low-income individuals more.

The vintage-based restriction is also more efficient at reducing equivalent emissions, decreasing NO_X emissions 55% more than simple restrictions. The improved emission reduction balances the higher surplus losses through a lower implied average cost of regulation, reducing it by €125,000/ton. The targeting effectiveness is more nuanced for the diesel-based

[16] For instance, in 2022, 82 German cites and 15 French cities are under low emission zone restrictions. Madrid, Barcelona, Milan, Rome, and Naples are additional examples of large cities with this type of policy. Source: https://urbanaccessregulations.eu/countries-mainmenu-147. Last accessed: 08/04/2022.

restriction: CO_2 emissions decrease less than in the standard restriction, but we observe larger reductions of local pollutants. The net emission benefits are identical under diesel and traditional driving restrictions (€0.28 million).

Table 15: Surplus changes under different driving restrictions.

	Standard	**Vintage-based**	**Diesel-based**
Total ΔCS (M€)	-1.11	-1.19	-1.03
ΔCS, constant speed	-1.28	-1.36	-1.18
ΔCS from speed	0.164	0.164	0.152
ΔW_2 = ΔCS + tax rev. - ΔE Total ΔwCS (M€)	-1.16	-1.37	-1.11
ΔCO_2 (ton)	-300	-363	-259
$\Delta eqNO_X$ (ton)	-1.24	-1.92	-1.36
Implied cost $eqNO_X$(€/ton)	897,728	621,314	756,039
% ΔCS > 0	0.075	28.9	32.2
% ΔCS < 0	79.7	50.8	47.6

Note:"ΔE" are changes in emissions valued at standard levels.

6.3 Improving public transport

While the main analysis focuses on traffic policies, we can provide insights on how improvements to public transport can mitigate consumer surplus losses. Public transport is the most used transportation mode in our data; however, 28.5% of the individuals do not have access to it. In the first scenario, we improve public transport coverage by allowing these individuals to use a hypothetical public transport service. We use the median characteristics of public transport: a speed of 14.6 km/hr, a price of €1.24, and congestion levels of 171% at peak hours and 80% at off-peak hours, two layovers and only using the railway system. In the second scenario, we decrease public transport travel times by 40%, similar to a frequency or speed improvement. Finally, in the third scenario, we make public transport free. We compare the effects of the variable toll with and without the three different public transport improvements. The quality improvement and the free usage increase the total public transport usage by around 10%. In contrast, the coverage improvement increases use by almost 30%, indicating that improving coverage is the best instrument to increase public transit ridership.

Surplus changes are shown in Table 16. Public transport improvements reduce consumer surplus losses by between 8% and 34%. The largest reduction corresponds to coverage improvements. All policies reduce car usage and therefore imply lower tax revenues. Moreover, reducing surplus losses does not compensate for the lower tax revenue, generating lower welfare gains across all scenarios. However, this welfare measure does not include public transport revenue, which would increase in the first two scenarios. The share of winners from the toll slightly increases due to the coverage improvement, rising to almost 19.6%. In addition, this policy considerably reduces the losses for the most affected individuals.

Table 16: Consumer surplus variation under public transport improvements.

	(1)	(2)	(3)	(4)
Total ΔCS (M€)	-0.691	-0.528	-0.475	-0.636
ΔCS, constant speed	-0.931	-0.797	-0.692	-0.842
ΔCS from speed	0.24	0.269	0.217	0.206
Total ΔwCS (M€)	-0.752	-0.57	-0.551	-0.689
Tax revenue (M€)	0.872	0.715	0.818	0.762
ΔW_1 = ΔCS + Tax revenue (M€)	0.181	0.187	0.343	0.126
ΔW_2 = ΔCS + tax rev. - ΔE (M€)	0.212	0.228	0.366	0.155
ΔCO_2 (ton)	-330	-440	-239	-312
$\Delta eqNO_X$ (ton)	-1.37	-1.82	-0.998	-1.31
Implied cost local pollutants (€/ton NO_X)				
W/o redist (€/ton)	502,556	289,501	475,596	485,850
With redist (€/ton)	-131,690	-102,474	-343,887	-96,116
% ΔCS > 0	18.9	20.8	28.8	18.1
% ΔCS < 0	60.8	59	50.9	61.6
Min ΔCS (€)	-4.07	-2.47	-3.93	-4.11
Max ΔCS (€)	0.766	0.78	1.02	0.672

Note: (1): Benchmark. (2): Coverage improvement. (3): Duration improvement. (4): Free access.

7 Discussion about the scope of the model

Our equilibrium transportation decision model is rich and provides interesting insights into the different policy effects. We focus here on predicting the impacts of simple policies that we have seen implemented in practice. However, our model could predict many more interesting counterfactual situations. Here, we outline a few counterfactuals that could be done and discuss their possible relevant assumptions.

Change in road congestion technology Recent urban policies consist of pedestrianization of specific roads, as well as their conversion into bike lanes. By reducing the road capacity for cars, such policies reduce speed for the same level of traffic. We can model such policies as changes in the congestion technologies, either through parallel shifts of the curves or a proportional decrease in speed along the curve. Alternatively, we could also model improvements of the road congestion technology, such as a road capacity increase or autonomous vehicles that would make traffic smoother.

Carpooling We have recently seen some initiatives to encourage carpooling. The U.S. has, for instance, a long tradition with high occupancy lanes in 27 metropolitan areas. While our model cannot predict the impacts of dedicating special lanes to carpooling and how individuals decide whether or not to carpool, we can still evaluate the benefits of carpooling under some simple assumptions. For instance, assuming that everyone has to carpool with three other people, a carpooling requirement amounts to considering that individuals are only driving one-fourth of their kilometers. Thus, it is equivalent to modifying the mapping parameter between individuals using their cars and the occupancy rate to $\tilde{\phi}^a = \phi^a/4$. The

model can easily accommodate different cost-sharing assumptions and include detours that increase driving times.

Modifying work conditions We could consider policies incentivizing working from home a fraction of the time. We can model this similarly to carpooling. For instance, if we assume individuals work from home one day per week, this is equivalent to reducing the expected number of kilometers driven by 20% or modifying the mapping parameter between the number of kilometers driven and the occupancy rate to $\tilde{\phi}^a = \frac{4}{5}\phi^a$. In addition, our model can be easily extended to more periods. This would allow us to consider policies like spreading work schedules that decrease the penalty for commuting outside peak hours and a more uniform distribution of congestion across time.

Parking cost and availability Recent literature shows the importance of parking prices and availability on traffic levels (Ostermeijer et al., 2022). The model can easily evaluate such policy through targeted increases in the costs of car trips.

8 Conclusion

Combining data from a detailed survey, Google Maps, TomTom, and passenger flow in railway public transit, we estimate a nested logit model to represent the transportation decisions of individuals for their daily trips to work or places of study in the Paris metropolitan area. The estimated parameters confirm the importance of trip duration for individual decisions and reveal profound schedule inflexibility making it challenging to discourage individuals from driving at peak hours. We combine this transportation mode choice model with a flexible reduced-form congestion model that predicts how road speeds vary when the number of drivers changes in the different parts of the city. We simulate the effects of simple transportation policies and measure their welfare effects on individuals and their impacts on emissions. We find that all the regulations are costly for individuals. Still, simple driving restrictions are not more costly for individuals than uniform road tolls because they force everyone to contribute to traffic reduction. As a result, it generates fewer surplus losses than uniform tolls on aggregate. However, variable tolls are better than driving restrictions because they target individuals with long distances and are thus efficient at reducing the total number of kilometers driven. In contrast, driving restrictions do not raise revenue, unlike tolls. If the toll revenue is entirely redistributed to individuals, moderate toll values may improve the total surplus.

References

Akbar, P. and G. Duranton (2017). Measuring the cost of congestion in highly congested city: Bogota. *CAF – Working paper*.

Allen, T. and C. Arkolakis (2022). The Welfare Effects of Transportation Infrastructure Improvements. *The Review of Economic Studies*.

Anderson, M. L. (2014). Subways, strikes, and slowdowns: The impacts of public transit on traffic congestion. *American Economic Review 104*(9), 2763–96.

Anderson, M. L. and L. W. Davis (2020). An empirical test of hypercongestion in highway bottlenecks. *Journal of Public Economics 187*, 104197.

Arnott, R., A. De Palma, and R. Lindsey (1990). Economics of a bottleneck. *Journal of Urban Economics 27*(1), 111–130.

Arnott, R., A. D. Palma, and R. Lindsey (1993). A structural model of peak-period congestion: A traffic bottleneck with elastic demand. *The American Economic Review 83*(1), 161–179.

Barahona, N., F. A. Gallego, and J.-P. Montero (2020). Vintage-specific driving restrictions. *The Review of Economic Studies 87*(4), 1646–1682.

Barwick, P. J., S. Li, A. R. Waxman, J. Wu, and T. Xia (2021). Efficiency and equity impacts of urban transportation policies with equilibrium sorting. Working paper, National Bureau of Economic Research.

Basso, L. J. and H. E. Silva (2014, November). Efficiency and substitutability of transit subsidies and other urban transport policies. *American Economic Journal: Economic Policy 6*(4), 1–33.

Batarce, M. and M. Ivaldi (2014). Urban travel demand model with endogenous congestion. *Transportation Research Part A: Policy and Practice 59*, 331 – 345.

Bento, A., K. Roth, and A. R. Waxman (2020). Avoiding traffic congestion externalities? The value of urgency. Working paper, National Bureau of Economic Research.

Bou Sleiman, L. (2021). Are car-free centers detrimental to the periphery? Evidence from the pedestrianization of the Parisian riverbank. Technical report, Center for Research in Economics and Statistics.

Buchholz, N., L. Doval, J. Kastl, F. Matějka, and T. Salz (2020). The value of time: Evidence from auctioned cab rides. Technical report, National Bureau of Economic Research.

Carstensen, C. L., M. J. Hansen, F. Iskhakov, J. Rust, and B. Schjerning (2022). A dynamic equilibrium model of commuting, residential and work location choices. *Topics in Urban Economics: Non-Market Valuation and Location*, 35.

COPERT methodology report (2020). Emep/eea air pollutant emission inventory guidebook 2019 - update oct. 2021. *EEA*.

Couture, V., G. Duranton, and M. A. Turner (2018). Speed. *Review of Economics and Statistics 100*(4), 725–739.

Davis, L. W. (2008). The effect of driving restrictions on air quality in Mexico City. *Journal of Political Economy 116*(1), 38–81.

De Palma, A. and R. Lindsey (2006). Modelling and evaluation of road pricing in Paris. *Transport Policy 13*(2), 115–126.

De Palma, A., R. Lindsey, and G. Monchambert (2017). The economics of crowding in rail transit. *Journal of Urban Economics 101*, 106–122.

De Palma, A., F. Marchal, and Y. Nesterov (1997). Metropolis: Modular system for dynamic traffic simulation. *Transportation Research Record 1607*(1), 178–184.

DG MOVE (2014). Update of the handbook on external costs of transport. *Report for the European Commission*.

Engelson, L. and M. Fosgerau (2016). The cost of travel time variability: Three measures with properties. *Transportation Research Part B: Methodological 91*, 555–564.

Galdon-Sanchez, J. E., R. Gil, F. Holub, and G. Uriz-Uharte (2021). Benefits and costs of driving restriction policies: The impact of Madrid Central on congestion, pollution and consumer spending. Working paper.

Gale, D. and H. Nikaido (1965). The jacobian matrix and global univalence of mappings. *Mathematische Annalen 159*(2), 81–93.

Gallego, F., J.-P. Montero, and C. Salas (2013). The effect of transport policies on car use: Evidence from Latin American cities. *Journal of Public Economics 107*, 47 – 62.

Geroliminis, N. and C. F. Daganzo (2008). Existence of urban-scale macroscopic fundamental diagrams: Some experimental findings. *Transportation Research Part B: Methodological 42*(9), 759 – 770.

Goldszmidt, A., J. A. List, R. D. Metcalfe, I. Muir, V. K. Smith, and J. Wang (2020). The value of time in the United States: Estimates from nationwide natural field experiments. Working paper, National Bureau of Economic Research.

Hall, J. D. (2018). Pareto improvements from lexus lanes: The effects of pricing a portion of the lanes on congested highways. *Journal of Public Economics 158*, 113–125.

Hall, J. D. (2021). Can tolling help everyone? estimating the aggregate and distributional consequences of congestion pricing. *Journal of the European Economic Association 19*(1), 441–474.

Hall, J. D. and I. Savage (2019). Tolling roads to improve reliability. *Journal of urban economics 113*, 103187.

Hang, D., D. McFadden, K. Train, and K. Wise (2016). Is vehicle depreciation a component of marginal travel cost?: A literature review and empirical analysis. *Journal of Transport Economics and Policy 50*(2), 132–150.

Hanna, R., G. Kreindler, and B. A. Olken (2017). Citywide effects of high-occupancy vehicle restrictions: Evidence from "three-in-one" in Jakarta. *Science 357*(6346), 89–93.

Haywood, L. and M. Koning (2015). The distribution of crowding costs in public transport: New evidence from Paris. *Transportation Research Part A: Policy and Practice 77*, 182–201.

Herzog, I. (2022). The city-wide effects of tolling downtown drivers: Evidence from London's congestion charge. Working papers.

Hintermann, B., B. M. Schoeman, J. Molloy, T. Götschli, A. Castro, C. Tchervenkov, U. Tomic, and K. W. Axhausen (2021). Pigovian transport pricing in practice. Technical report, WWZ Working Paper.

Jia, Z., C. Chen, B. Coifman, and P. Varaiya (2001). The PeMS algorithms for accurate, real-time estimates of g-factors and speeds from single-loop detectors. In *ITSC 2001. 2001 IEEE Intelligent Transportation Systems*, pp. 536–541. IEEE.

Kilani, M., S. Proost, and S. Van der Loo (2012). Tarification des transport individuels et collectifs à Paris. rapport final de recherche PREDIT. In *Technical Report*.

Kilani, M., S. Proost, and S. Van der Loo (2014). Road pricing and public transport pricing reform in Paris: Complements or substitutes? *Economics of Transportation 3*(2), 175–187.

Kreindler, G. E. (2022). Peak-hour road congestion pricing: Experimental evidence and equilibrium implications. *Working paper*.

Li, S. (2018). Better lucky than rich? Welfare analysis of automobile licence allocations in Beijing and Shanghai. *The Review of Economic Studies 85*(4), 2389–2428.

Loder, A., L. Ambühl, M. Menendez, and K. W. Axhausen (2017). Empirics of multi-modal traffic networks–

using the 3D macroscopic fundamental diagram. *Transportation Research Part C: Emerging Technologies 82*, 88–101.

Mangrum, D. and A. Molnar (2020). The marginal congestion of a taxi in new york city. Technical report.

McFadden, D. (1974). The measurement of urban travel demand. *Journal of public economics 3*(4), 303–328.

Ostermeijer, F., H. Koster, L. Nunes, and J. van Ommeren (2022). Citywide parking policy and traffic: Evidence from amsterdam. *Journal of Urban Economics 128*, 103418.

Parry, I. and K. Small (2009). Should urban transit subsidies be reduced? *American Economic Review 99*(3), 700–724.

Reynaert, M. and J. M. Sallee (2021). Who benefits when firms game corrective policies? *American Economic Journal: Economic Policy 13*(1), 372–412.

Rosaia, N. (2020). Competing platforms and transport equilibrium: Evidence from new york city. Technical report.

Russo, A., M. W. Adler, F. Liberini, and J. N. van Ommeren (2021). Welfare losses of road congestion: Evidence from rome. *Regional Science and Urban Economics 89*, 103692.

Small, K. A. (2012). Valuation of travel time. *Economics of transportation 1*(1-2), 2–14.

Small, K. A., E. T. Verhoef, and R. Lindsey (2007). *The economics of urban transportation*. Routledge.

Small, K. A., C. Winston, and J. Yan (2005). Uncovering the distribution of motorists' preferences for travel time and reliability. *Econometrica 73*(4), 1367–1382.

Tarduno, M. (2022). For whom the bridge tolls: Congestion, air pollution, and second-best road pricing. Working papers.

Tassinari, F. (2022). Low emission zones and traffic congestion: evidence from Madrid Central. Technical report.

Train, K. E. (2009). *Discrete choice methods with simulation*. Cambridge university press.

Tsivanidis, N. (2022). The aggregate and distributional effects of urban transit infrastructure: Evidence from Bogota's TransMilenio. Working paper.

Van Den Berg, V. and E. T. Verhoef (2011). Winning or losing from dynamic bottleneck congestion pricing?: The distributional effects of road pricing with heterogeneity in values of time and schedule delay. *Journal of Public Economics 95*(7), 983–992.

Yang, J., A.-O. Purevjav, and S. Li (2020). The marginal cost of traffic congestion and road pricing: Evidence from a natural experiment in Beijing. *American Economic Journal: Economic Policy 12*(1), 418–53.

Appendix (for online publication only)

A Additional results on the uniqueness of the model equilibrium

We provide here the proofs of uniqueness of equilibrium under special cases of our model and investigate the numerical properties of our algorithm for the general model.

A.1 Special cases

A.1.1 One period, one area

We consider here the case of only one endogenous speed in the model. The equilibrium speed v is given by:

$$v - f(\phi \sum_{n=1}^{N} \omega_n s_n(v) k_n + \gamma) = 0$$

We define $g(v) := v - f(\phi \sum_{n=1}^{N} \omega_n s_n(v) k_n + \gamma)$. If the non-linear equation admits a solution, the solution is unique if the function is monotonic, i.e., if $|g'(v)| > 0 \; \forall v \in [\underline{v}, \overline{v}]$. The derivative is:

$$g'(v) = 1 - \underbrace{f'(\phi \sum_{n=1}^{N} \omega_n s_n(v) k_n + \gamma)}_{\leq 0} . \underbrace{\phi}_{>0} . \sum_{n=1}^{N} \omega_n k_n \underbrace{\frac{\partial s_n(v)}{\partial v}}_{\geq 0},$$

which is always positive for $v \in [\underline{v}, \overline{v}]$ as long as the speed function is weakly decreasing in the occupancy rate and the probability to drive increases with the speed.

A.1.2 Multiple periods, one area

Now, we consider a model with a single area but multiple time periods which are substitutes for individuals. In this setting we have a system of T non-linear equations, $\mathbf{g}(\mathbf{v}) = 0$, where:

$$g_t(\mathbf{v}) := v_t - f\left(\phi_t \sum_{n=1}^{N} \omega_n k_n s_{nt}(\mathbf{v}) + \gamma_t\right)$$

We want to show that the Jacobian of the system is a Leontieff matrix, i.e. the diagonal terms are positive and the off-diagonal terms are non-positive. First we compute the diagonal

terms, which resemble the previous derivative and is always greater than 1:

$$\frac{\partial g_t}{\partial v_t} = 1 \underbrace{-f'(\phi_t \sum_{n=1}^{N} \omega_n k_n s_{nt}(\mathbf{v}) + \gamma_t)}_{\geq 0} \cdot \underbrace{\phi_t}_{>0} \cdot \sum_{n=1}^{N} \underbrace{\omega_n k_n \frac{\partial s_{nt}(\mathbf{v})}{\partial v_t}}_{\geq 0}.$$

Then we compute the off-diagonal terms, which are always negative due to the substitutability between the different time periods:

$$\frac{\partial g_t}{\partial v_{t'}} = \underbrace{-f'(\phi_t \sum_{n=1}^{N} \omega_n k_n s_{nt}(\mathbf{v}) + \gamma_t)}_{\geq 0} \cdot \underbrace{\phi_t}_{>0} \cdot \sum_{n=1}^{N} \underbrace{\omega_n k_n \frac{\partial s_{nt}(\mathbf{v})}{\partial v_{t'}}}_{\leq 0}.$$

The Jacobian of $\mathbf{g}(\mathbf{v})$ is thus a Leontieff matrix and by Theorem 5 from Gale and Nikaido (1965) it is a P-matrix. We can then apply the main theorem of Gale and Nikaido (1965) (Theorem 1) that states that if the Jacobian of a system of non-linear equations is a P-matrix, the system has a unique solution in its bounded support.

A.2 General model

We provide here the analytical formula for the Jacobian of the contraction defined as:

$$g_t^a(\mathbf{v}, \kappa) = \kappa . v_t^a + (1 - \kappa) . f^a(\mathbf{v}).$$

We can separate the Jacobian in three types of derivatives: $\frac{\partial g_t^a(\mathbf{v},\kappa)}{\partial v_t^a}$, $\frac{\partial g_t^a(\mathbf{v},\kappa)}{\partial v_t^{a'}}$, $\frac{\partial g_t^a(\mathbf{v},\kappa)}{\partial v_{t'}^{a'}}$.

$$\frac{\partial g_t^a(\mathbf{v},\kappa)}{\partial v_t^a} = \kappa + (1 - \kappa) \underbrace{f^{a'}\left(\phi^a \sum_{n=1}^{N} \omega_n k_n^a s_{nt}(\mathbf{v}) + \gamma^a\right)}_{\leq 0} \cdot \underbrace{\phi^a}_{>0} \cdot \sum_{n=1}^{N} \underbrace{\omega_n k_n^a \frac{\partial s_{nt}(\mathbf{v})}{\partial v_t^a}}_{\geq 0}$$

$$\frac{\partial g_t^a(\mathbf{v},\kappa)}{\partial v_t^{a'}} = (1 - \kappa) \underbrace{f^{a'}(\phi^a \sum_{n=1}^{N} \omega_n k_n^a s_{nt}(\mathbf{v}) + \gamma^a)}_{\leq 0} \cdot \underbrace{\phi^a}_{>0} \cdot \sum_{n=1}^{N} \underbrace{\omega_n k_n \frac{\partial s_{nt}(\mathbf{v})}{\partial v_t^{a'}} \mathbb{1}\{k_n^{a'} > 0\}}_{\geq 0}$$

$$\frac{\partial g_t^a(\mathbf{v},\kappa)}{\partial v_{t'}^{a'}} = (1 - \kappa) \underbrace{f^{a'}(\phi^a \sum_{n=1}^{N} \omega_n k_n^a s_{nt}(\mathbf{v}) + \gamma^a)}_{\leq 0} \cdot \underbrace{\gamma^a}_{>0} \cdot \sum_{n=1}^{N} \underbrace{\omega_n k_n^a \frac{\partial s_{nt}(\mathbf{v})}{\partial v_{t'}^{a'}} \mathbb{1}\{k_n^{a'} > 0\}}_{\leq 0}$$

The signs of the derivatives of the probabilities are obtained from the analytical formulas

$$\frac{\partial s_{nt}(\mathbf{v})}{\partial v_{t'}^{a'}} = \underbrace{\frac{k_n^{a'}}{(v_{t'}^{a'})^2} \times \varepsilon_{nt'} \times 60}_{\geq 0} \times \underbrace{\frac{\beta_n^{\text{duration}}}{\text{duration}_n}}_{\leq 0} \times \underbrace{s_{nt}\left((1-\sigma)\frac{s_{n,t'}}{\sum_{\tilde{t}=1}^{T} s_{n\tilde{t}}} + \sigma s_{nt'}\right)\mathbb{1}\{k_n^{a'} > 0\}}_{\geq 0} \text{ if } t \neq t'$$

$$\frac{\partial s_{nt}(\mathbf{v})}{\partial v_{t}^{a'}} = \underbrace{-\frac{k_n^{a'}}{(v_{t}^{a'})^2} \times \varepsilon_{nt} \times 60}_{\leq 0} \times \underbrace{\frac{\beta_n^{\text{duration}}}{\text{duration}_n}}_{\leq 0} \times \underbrace{s_{nt}\left(1-(1-\sigma)\frac{s_{n,t}}{\sum_{\tilde{t}=1}^{T} s_{n\tilde{t}}} - \sigma s_{nt}\right)\mathbb{1}\{k_n^{a'} > 0\}}_{\geq 0}$$

B Additional information on data and sample construction

B.1 Information about the data

The EGT consitute publicly available data on demand on ADISP.[17] The survey was conducted from 2009 to 2011 between October and May, excluding school holidays. The region was divided into 112 sectors, where between 400 and 500 individuals were interviewed. In addition, instead of relying on a trip diary where surveyed individuals self-report their trips, the EGT relies on pollsters visiting households and recording the information of the trips performed the previous day.

The initial data contains 35,175 individuals and 124,262 trips. In our final sample, we keep work and study-related trips and only the first trip of the day. We drop trips if one of the variables we need for the model is missing (origin, destination, departure time, professional activity, residence location, or income class). We also drop trips using less common transportation modes that are not included in our choice set (e.g. taxis, boats) or individuals who took their first work trip outside the morning time window (generously defined as 4:00 a.m.- 3:00 p.m.). This leaves us with a final sample of 12,975 individuals.

The survey maps the Paris region into a grid with 1,489,347 squares to locate individual trips' origins and destinations. Each square is 100 square meters. Thus, we use the GPS coordinates of the centroids of the grid squares. This approach limits any trip geocoding inaccuracy to a maximum of approximately 70 meters.

Google Maps and TomTom Directions APIs provide directions and expected travel times associated with a given origin and destination pair of GPS coordinates at a specified departure time. The data from these API services have been used previously in the transportation

[17] Enquête Globale Transport (EGT) - 2010, DRIEA, ADISP, see http://www.progedo-adisp.fr/.

literature (see Kreindler, 2022, Hanna et al., 2017, Akbar and Duranton, 2017, and Tarduno, 2022). We use TomTom data for driving times because this API gives 2,500 free queries daily.

The public transport queries were done on June 2nd, 2019, setting all trips to take place on Tuesday, June 4th, 2019, with a departure time at 9:30 a.m. The car queries were done in April 2021, setting the trips to take place the Thursday 16th of September 2021 at 8:30 a.m. for peak hours and 6:30 a.m. for off-peak hours.

TomTom queries for future dates use historical trip data and not the live conditions. We may be worried that TomTom modified its prediction algorithm because of Covid. To solve concerns regarding the impact of Covid on traffic and TomTom's predictions, we compare our TomTom queries at peak hours (8:30 a.m.) with Google maps queries done in August 2019. We find that the average difference between the two data sources implies that TomTom queries predict trip durations 7.5% larger than the older ones from Google maps, with a median difference of 7.6%. The results suggest that the Covid crisis did not significantly decrease traffic and affected the prediction algorithm of TomTom. Furthermore, they show the similarities between the two sources and thus TomTom's reliability.

B.2 Car fuel consumption and emissions

B.2.1 Baseline estimation method

The EGT data do not include the information for car fuel consumption and emissions, so we rely on a prediction model. Since fuel consumption and car emissions are linked through the formula:

$$\mathrm{CO}_{2j} = fc_j \times ft_{k(j)},$$

where fc_j is the fuel consumption (in liter/km) for car j and $ft_{k(j)}$ reflects the quantity of CO_2 emissions in a liter of fuel and is equal to 2,287 g/L for gasoline cars and 2,686 g/L for diesel cars. We thus predict car CO_2 emissions and obtain the fuel consumption using the above formula. Our prediction model includes the following explanatory variables: fuel type, horsepower, a linear time trend, and the emission standards applicable at that time. To estimate this prediction model, we use car registration data in the Paris metropolitan area from 2003 to 2018 that contain the main car characteristics, sales, and the value of CO_2 emissions.[18]

We complement these data with local pollutant emissions data by car model from the UK Vehicle Certification Agency.[19] Note that the emissions data are all from official car

[18]These are proprietary data obtained from the French Car Manufacturers syndicate "CCFA" (for 2003-2008) and AAAData (for 2009-2018).

[19]Source: https://carfueldata.vehicle-certification-agency.gov.uk/downloads/archive.aspx

manufacturer tests and may be different from real-time driving emissions, as pointed out by Reynaert and Sallee (2021).

We first match the French car registration data to the UK emissions data so that we can weigh each car model in the UK emissions data by their sales in Paris metropolitan area in the prediction model. The two datasets do not contain the same car characteristics, so we rely on the following matching algorithm:

1. We compute the total car sales by year, brand, model name, fuel type, and CO_2 emissions in the French data.

2. We merge them with the UK emissions data by year, brand, model name, and fuel type. Since there are several versions for the same combination in the UK data, we select the closest neighbor based on cylinder capacity and CO_2 emissions. We use the following formula to compute the distance to every potential match:

$$\text{distance} = \sqrt{\left(\frac{\text{CO}_{2,FR} - \text{CO}_{2,UK}}{\text{CO}_{2,FR}}\right)^2 + \left(\frac{\text{Cylinder}_{FR} - \text{Cylinder}_{UK}}{\text{Cylinder}_{FR}}\right)^2}$$

3. To ensure the matching accuracy, we drop observations for which either the percentage difference in CO_2 emissions or cylinder capacity between the two matches is larger than 10%.

4. For each pollutant, we drop car models for which the emission levels are above the corresponding Euro standard limit. We also drop cars whose emissions are lower than a tenth of the Euro norm value, as they probably correspond to reporting errors.

For hybrid cars and other fuel types (liquefied petroleum or natural gas), we observe that the top models in France are not available in the UK emissions data. Thus, we rely on another dataset that provides car emissions data from 2012 to 2015. The data come from the French environment agency ("ADEME").[20] We follow the same procedure described above but allow for more discrepancy between the potential matches. Specifically, we drop observations only if the percentage difference in CO_2 emissions or cylinder capacity between the two matches is above 30%. We also rely on these ADEME data to obtain estimates of PM emissions for gasoline cars since the UK data only provide PM emissions for diesel cars.

[20] Source: https://www.data.gouv.fr/fr/datasets/emissions-de-co2-et-de-polluants-des-vehicules-commercialises-en-france/. We prefer not to use it for conventional fuel cars because the sample period is limited to the latest emission standards.

Once we have a final sample of car models with their corresponding sales and emissions, we estimate a prediction model. We specify the emissions level of a specific pollutant as a linear function of the horsepower, a linear time trend, and dummies for the years of changes in the emissions standard of this particular pollutant. We allow the parameters to be different by fuel type. Finally, we regress the logarithm of the emission levels on car characteristics for PM emissions because PM data are less reliable and have more outliers. All regressions are weighted by the car model sales. Given the small matched sample size (91 observations) for hybrid cars and other fuels, we do not estimate a prediction model and instead use the sales-weighted average emission levels by fuel type. Emissions for electric vehicles are set to zero for all pollutants. For some individuals in EGT data, the car vintage and horsepower are missing; in such cases, we attribute the average vintage or horsepower values in the EGT sample conditional on the fuel type.

Table 17: Fit of the prediction models and comparison between observed and predicted emissions.

	Gasoline				Diesel			
Pollutant	**R^2**	**Observed**	**Predicted**	**Predicted Copert**	**R^2**	**Observed**	**Predicted**	**Predicted Copert**
CO_2	0.84	203.1	197.1		0.83	171.4	167.5	
NO_X	0.31	100	62.1	87.9	0.78	370.5	345.6	568.8
HC	0.51	100	88.2	29.2	0.14	114.4	55.5	14.3
PM	0.85	0.44	1.59	1.9	0.85	3.26	23.1	30.2

Note: For PM emissions, we obtain the same R^2 for diesel and gasoline since the estimation is performed on pooled data. 'Observed average emissions' are calculated on the CCFA data for the year 2003 (the average car vintage in the EGT sample) except for PM. For PM emissions, we use the earliest year with available data: 2012 for gasoline and 2005 for diesel. 'Predicted' average emissions are computed on the EGT data using survey weights. For the Copert methodology we assume a speed of 45 km/hr.

B.2.2 Alternative method for emissions estimates

We follow an alternative method to estimate car emissions of local pollutants that depend on driving speed. We rely on Copert emissions factors for cars published in the COPERT methodology report (2020).[21] This report provides emission functions that link a car's emissions of local pollutants with its speed depending on fuel type, emission standard, and car segment (in four categories: mini, small, medium, and large).

The EGT data does not directly provide the car segments, so we predict them from the fiscal horsepower. We use our proprietary car data containing the horsepower and segment for each car in the choice set from 2003 to 2018. We specify an ordered logit model to predict the car segment from its horsepower. More specifically, we consider:

$$\mathbb{1}(C_i = c_k) = \mathbb{1}\left(n_k \leq h_i + \eta_i \leq n_{k+1}\right),$$

[21] See https://www.emisia.com/utilities/copert/documentation/.

where C_i is the segment of car model i and $c_k = c_1, ...c_K$ are the different possible segments ordered from the smallest to the largest. h_i is the observed horsepower of the car, and η_i is a random error that we assume to follow a logistic distribution. Finally, $n_k = n_1, ...n_{K-1}$ are the segment threshold that we want to estimate. The probability that car i belongs to segment c_k can be expressed as:

$$
\begin{aligned}
&P(C_i = c_1) = P(h_i + \eta_i \leq n_1) = F_\eta(n_1 - h_i) \\
&P(C_i = c_k) = P(h_i + \eta_i \geq n_{k-1} \;\&\; h_i + \eta_i \leq n_k) = F_\eta(n_k - h_i) - F_\eta(n_{k-1} - h_i) \quad \text{for } k \in [2, K-1] \\
&P(C_i = c_K) = P(h_i + \eta_i \geq n_{K-1}) = 1 - F_\eta(n_{K-1} - h_i)
\end{aligned}
$$

We estimate the parameters $n_k = n_1, ..., n_{K-1}$ by maximum likelihood.

Additionally, we assign cars to an emission standard from their vintage: cars with a vintage below 2000 are under Euro 2 standards. From 2000 to 2005 they are under Euro 3 standards. From 2005 onward, they are subject to Euro 4 standards. Since both the Copert emissions data and the EGT data include information on fuel types, we can directly match survey cars to the correct set of factors by fuel type. We assume electric vehicles do not emit pollutants.

B.3 Cost estimation

The survey does not report the costs incurred by the individuals, so we estimate them. For all transportation modes, we neglect the fixed expenses. Thus, expenses like car purchase price, insurance, taxes, or parking costs, are not included in our estimates. The rationale is that we focus on the short-term reaction to policy introduction, implying that individuals cannot avoid these fixed costs. Moreover, walking is always free, while cycling is free only for households that own bicycles. If the individual has an annual bike-sharing subscription, the subscription cost is divided by 730, equivalent to assuming two bike trips per day. In other cases, we consider biking has the price of a single bike-sharing ticket, €1.7.

B.3.1 Public transport

Public transport in Paris comprises a network operated by two companies: "RATP" mainly covers the public transport inside Paris and close suburbs, and "SNCF" operates trains connecting Paris to the suburban areas. During our data period, the RATP pricing system relies on five pricing zones of the trip's origin and destination. We use the prices stated in the price guide of RATP for July 2011.[22] In contrast, the ticket price using the SNCF network depends on the exact stations of origin and destination rather than zones. Since there is no

[22]Source: "Guide tarifaire", Juillet 2011, https://www.slideshare.net/quoimaligne/guide-tarifaire-ratp-sncf-ile-de-france-2011.

exhaustive data on the prices for all combinations of origin and destination train stations, we rely on a sample of ticket prices for 36 origin and destination pairs and estimate the train ticket price as a cubic function of the distance between stations. This regression has a good fit with an R^2 of 0.82. We use this function to predict prices for all origin-destinations pairs in the SNCF network.

For individuals with a public transport subscription, we estimate a trip's average cost by dividing the daily price of the subscription by two, which is the average number of trips taken in a day conditional on using public transport. For individuals without a subscription, missing information about their subscription coverage, or taking a trip outside their subscription coverage, we assume they pay the regular ticket price. Seven individuals stated to have used the service without paying (fraud); we attribute a zero cost for these trips. The survey includes information on whether individuals can buy subsidized or reduced-price tickets or subscriptions; we use this information when computing the cost of public transport.

B.3.2 Cars and motorcycles

We estimate the cost of using a car or a motorcycle by combining the trip distance from the itinerary provided by TomTom, estimates of the fuel consumption of household vehicles, and average fuel prices in 2011 from the National Survey Institute ("Insee").[23] For motorcycles, we assign the average fuel consumption by the number of cylinders, which is the only motorcycle characteristic we observe in the EGT data .[24] When a household has multiple vehicles, we assume the trip uses the most fuel-efficient one. We also assume each individual pays the total cost of the trip, regardless of the number of passengers.

B.4 Public transport overcrowding

We first compute a line-level measure of overcrowding in public railway transport. To do so, we rely on data provided by SNCF and RATP on the number of passengers at the metro or train station level. We use data for 2015, the oldest data available, and consider only the urban railway network, where overcrowding is the most problematic. The data only record the validations from passengers that use an electronic metro card; there is no exhaustive data on passengers using tickets. Estimates suggest that the electronic validations represent two-thirds of the traffic for 2016; during morning peak and off-peak hours, the share should

[23] Source for fuel prices: https://www.prix-carburants.developpement-durable.gouv.fr/petrole/se_cons_fr.htm.

[24] Source: French Energy Agency ("ADEME"). See https://www.statistiques.developpement-durable.gouv.fr/les-deux-roues-motorises-au-1er-janvier-2012.

be even higher.[25] We exploit the variation between peak and off-peak hours traffic across metro lines to estimate the role of overcrowding in transportation decisions. As long as traffic is homogeneously underestimated over the network and periods, omitting a portion of the traffic is not a major problem.

The data are composed of two separate datasets. The first contains daily entry flows of passengers at the railway station level. The second dataset contains "hourly profiles" at the station level: the distribution of validations (in %) across hours for different periods (business days outside holidays, business days during school holidays, and weekends).[26] By combining these datasets, we obtain daily estimates of the number of passengers in each metro station for regular business days. We exclude weekends, school holidays, public holidays, and two dates with a relatively low total number of entries.[27] In the end, we average traffic levels over 172 days. We use the passenger flow between 7:00-8:59 a.m. to represent peak hours and 6:00-6.59 a.m. for off-peak hours. We observe the number of passengers entering each station, but not the line they take. Thus, we allocate passengers to metro lines proportionally, using the annual traffic levels by lines as weights.

We also use schedule data that provide frequencies of trains at the station level for September 2015.[28] We average across stations to get the expected number of trains for each railway line. Additionally, we gather information about the passenger capacity of the train models used on each line.[29] The passenger capacity represents the number of passengers a train can carry, assuming four passengers per square meter. We compute the total railway line passenger capacity each period by multiplying the train capacity by the number of trains per hour. Finally, the overcrowding level c_{lt} for line l, at period t is:

$$c_{lt} = \frac{p_{lt}}{2 \times tc_{lt}},$$

where p_{lt} is the hourly number of passengers in line l at time period t, tc_{lt} is the line total passenger capacity per hour. Since there are two directions, we multiply the total line capacity by two and use the total number of passengers going in both directions. Finally, we obtain individual overcrowding levels by weighting the overcrowding level of each line

[25] See https://www.iledefrance-mobilites.fr/usages-et-usagers-des-titres-de-transport.

[26] We use the average profiles for the business days outside holidays for the second semester of 2015 since we noticed some problems with the data from the first semester 2015: the percentages did not sum to 100% for 20 stations.

[27] These record total daily traffic levels below a million, while the average is 7.5 million according to the official figures of the RATP. We interpreted this low number of passengers as indicating the occurrence of a strike.

[28] 'General Traffic Feed Specification', see: https://transitfeeds.com/l/162-paris-france.

[29] We rely on Wikipedia and internal reports from the transport organization in the Paris area "STIF" containing information about the fleet of trains.

used in a trip by the time spent in that line. Finally, we provide in Table 18 the estimates of the overcrowding levels in the different metro and train lines. On average, we estimate the overcrowding to be 0.89 at off-peak hours and 1.43 at peak hours. But these averages hide substantial heterogeneity across lines that provide key variations for estimating the sensitivity to overcrowding in public transport.

Table 18: Estimates of overcrowding levels in the railway public transit.

Metro			Suburb trains		
Line	**Off-peak**	**Peak**	**Line**	**Off-peak**	**Peak**
1	0.43	0.72	A	2.35	4.37
2	0.5	0.77	B	0.55	1.07
3	1.04	1.29	C	0.58	1.16
3B	0.18	0.36	D	1.24	1.75
4	0.6	1.11	E	0.78	1.37
5	1.3	1.84	H	0.4	0.71
6	0.72	1.01	J	0.63	1.12
7	1.5	1.71	K	1.39	2.22
7B	0.19	0.41	L	0.61	1.36
8	0.86	1.12	N	0.48	1.01
9	0.81	1.07	P	1.91	3.82
10	0.59	1.13	R	0.93	1.3
11	0.98	1.39	U	0.88	2.1
12	1.07	1.44			
13	1.62	1.93			
14	0.56	0.95			

B.5 Real estate values

We proxy household wealth using expected housing values. To estimate each household's real estate price, we rely on a database containing all real estate transactions in France for 2014-2015 from the French tax authority and CEREMA.[30] We use this period since it is the earliest for which these data are publicly available.

We match each household to all the estate transactions from the municipality of residence and the neighboring municipalities. For Paris, we use the "arrondissement" level.[31] We limit the sample of matches to apartment and house sales and properties sold in one transaction and exclude partial sales of property. We drop transactions with a price of zero or above five million euros and keep only the properties with a built surface between 15 and 500 square meters. We then compute the average price per square meter for each transaction by dividing the price by the property's built surface. Next, we trim the sample and drop the top 0.5 % and the bottom five percent of each municipality's distribution of square meter prices.

[30]("Demande de Valeurs Foncières - DFV+", see https://www.data.gouv.fr/fr/datasets/dvf-open-data/#_.

[31]Paris is split in 20 smaller units called "arrondissements".

Next, we estimate individual estate prices by taking a weighted average over all transactions from the municipality and the neighboring municipalities, using the inverse distance between the household and the match as weight. We finally multiply the average estate price by the household surface area reported in the EGT survey. As seen in Table 19, the average real estate price that we estimate for each area is close to the area-specific price from external sources, supporting the credibility of our estimates.

Table 19: **Comparison of the real estate prices.**

	Paris	**Close suburbs**	**Far suburbs**
Average from our estimates	8,030	4,789	3,175
Average from official data	8,074	4,338	2,998

Note: in €/m². Our average is computed using survey weights. Average from official data obtained by averaging quarterly average prices for the year 2014. Source: https://basebien.com/PNSPublic/DocPublic/Historiquedesprixdesappartementspardep.pdf

B.6 Descriptive statistics of the final sample

Table 20 provides a comparison between the durations and costs for the transportation modes available to each individual. Taking the car is the fastest option and available to the largest fraction of individuals. Still, the low initial shares suggest that the high monetary cost dissuades many from choosing it. Interestingly, public transport is not the fastest nor the cheapest alternative on average, yet 45% of the individuals choose it in the sample. The public transport cost does not increase much with distance while the car or motorcycle costs linearly increase with distance. For this reason, the maximum price of public transport is lower than the maximum car and motorcycle costs.

Table 20: Average duration, cost and availability by transportation mode.

Variable	Mean	Median	Std. dev.	Min	Max
Duration					
Bike	52.1	39.6	40.7	0.57	150
Public transport	46.9	41.7	26.9	4.1	279
Motorbike	17.7	15.6	12.4	0.72	93.8
Walk	64.8	54.5	38.6	1.54	150
Car, peak	26.6	21	20.6	0.87	124
Car, off-peak	20.4	16.5	16	0.73	126
Cost					
Bicycle	0.64	0	0.82	0	1.7
Public transport	1.25	1.24	1.27	0	10.55
Motorcycle	1.21	0.72	1.39	0	13.72
Car	1.17	0.76	1.25	0	14.24
	Mode availability			**Shares**	
Bicycle	69.94			2.08	
Public transport, peak	71.54			30.33	
Public transport, off-peak	71.54			14.52	
Motorcycle	12.85			2.08	
Walk	42.72			15.8	
Car, peak	79.75			22.88	
Car, off-peak	79.75			12.31	

Note: Durations in minutes, costs in €. Mode availability and initial shares in %.

C Additional estimation results

C.1 Robustness checks for the transportation mode choice model

We first analyze the robustness of our estimates to several model assumptions. We provide the estimates of the average utility parameters in Table 21 and the implied values of travel time in Table 22.

Weather controls We use historical hourly data from OpenWeather for the city of Paris to control for the possible role of weather on individual choices.[32] First, we match the OpenWeather data to the exact departure hour and date provided in the survey. Then, based on the distribution of temperatures in our sample, we construct temperature quintiles. For rain and snow, we create four categories based on the levels (in millimeter per hour): 0, less than 0.3, between 0.3 and 0.8, and more than 0.8. The weather dummies are then interacted with the bike and walk alternative constants, as these modes are the most susceptible to being affected by the weather shocks. From the results, we can see that the inclusion of weather controls has no significant impact on the average sensitivities to duration and cost and almost no impact on the distribution of valuations of travel time.

[32]Source for weather data: https://openweathermap.org/.

Travel time reliability Recent transportation literature has focused on the importance of the reliability of travel time for individual transportation decisions (Hall and Savage, 2019, Bento et al., 2020, Engelson and Fosgerau, 2016, Small et al., 2005). We study the role of preferences for travel time reliability in our model and how including this factor affects our estimates. We build a measure of travel time reliability by collecting real-time traffic data from TomTom for all trips in our sample for every weekday between June 13$^{\text{th}}$, 2022, and June 30$^{\text{th}}$, 2022. We query trip itinerary and durations at 6:30 a.m. (to represent off-peak hours) and at 8:30 a.m. (for peak hours). We construct a proxy of reliability by taking the standard deviation of the durations for each trip at each period.[33]. As seen from the estimation results, the average utility parameters remain close to the benchmark, and the distribution of the values if travel time is marginally modified.

Car depreciation cost In the benchmark model, we consider the cost of a car trip to be determined only by its fuel cost and potential road tolls. Here, we consider an alternative cost definition that includes the car's depreciation cost, in the spirit of Hang et al. (2016). Using the CCFA and AAAdata data for 2003-2011, we regress car prices on fiscal power and fuel type and use the estimated coefficients to predict car prices for all the cars in our EGT sample. To get the average trip depreciation rate for each vehicle, we assume the car's price is uniformly amortized over twelve years. Then, the yearly cost is divided by 506, equivalent to taking two trips per workday (253 workdays per year). This gives us the average depreciation cost per trip. The depreciation cost is, on average, 11.5 times larger than the trip's fuel cost, with an average depreciation cost of €3.45, translating into a sharp decrease in individual sensitivity to cost. We find that the average VOT is €36.8, amounting to 154% of the average wage in Paris in 2011 (€23.9), very different from what the literature on VOT suggests.

Unobserved preference heterogeneity We consider three extensions of the benchmark specification that allow for unobserved heterogeneity in the sensitivity to duration, cost, and the off-peak hour dummy. We thus estimate three random coefficient versions of the benchmark model, assuming that the random coefficients follow a normal distribution. We find non-significant unobserved heterogeneity in the sensitivity to trip duration and the off-peak hour dummy. This result is probably the consequence of including multiple demographic interactions in the benchmark specification. However, we estimate a significant coefficient for the heterogeneity in the trip's cost. Since the standard deviation of the cost sensitivity is

[33]We also consider another reliability measure given by the difference between the 80$^{\text{th}}$ and 50$^{\text{th}}$ percentiles as suggested by Small et al. (2005). We choose to rely on the standard deviation because we obtain a better fit

relatively large, a considerable fraction of individuals has either a positive or close to zero cost sensitivity, which is inconsistent with our model. This specification, in turn, generates unrealistic extreme valuations of travel time.

Specification for the duration We study different functional form assumptions regarding the role of the trip's duration in the utility. We consider utility to be linear in duration instead of the logarithm of duration, as well as a model with a third degree polynomial on duration, in the spirit of Small et al. (2005) who specify individual preferences as a polynomial of distance interacted with duration. The estimates of the values of travel time are rather sensitive to the assumed functional form. Using the logarithm of duration allows shorter trips to have a larger disutility from additional travel. Forcing the disutility from travel time regardless of the trip length considerably reduces all the values of travel time. With the third-degree polynomial of duration, we obtain a much wider distribution of the opportunity costs of time than in our benchmark model, but the median value is close to our average. In addition, we find some negative valuations for trip duration, which is inconsistent with our model.

Alternative model assumptions We consider several alternative model specifications to check the robustness of our model estimates to different assumptions. First, we consider an alternative definition of off-peak hours driving durations. Instead of using only the 6:30 a.m. durations for the off-peak car alternative, we take the average duration between the TomTom queries at 6:30 a.m. and 9:30 a.m. This change has minimal effects on the average coefficients and almost no impact on the distribution of the values of travel time.

Second, we estimate a model with three periods: early off-peak hours (departure before 7:00 a.m.), peak hours (departure between 7:00-8:59 a.m.), and late off-peak hours (after 9:00 a.m.). The distribution of the values of travel time indicates slightly lower average and median values. We indeed estimate a larger sensitivity to the trip cost as Column (9) of Table 21 shows.

We also consider a model where we modify the nest structure by allowing individuals to choose first between peak and off-peak hours and then choose the transportation mode. This model allows for correlation in the preference shocks across all the alternatives within a departure time. However, column (10) of table 21 shows a high value for the nest parameter (σ), indicating that the options within nests are almost independent and suggesting that our nesting structure is more relevant.

Finally, we consider two possible changes to our choice set definition. First, we allow every

individual to drive, even those who do not own a car. For those without a car, we attribute the average car cost in the sample. Then, we query the TomTom service for those trips for the travel times, as with the rest of the sample. As expected, adding a non-available alternative changes the results by lowering the average utility of driving. However, the sensitivities to cost and duration are not affected very much. We would still obtain slightly higher values of travel times. The second change in the choice set definition that we study corresponds to allowing only individuals who have a bike or a bike-sharing pass to use this mode. We see very few changes, in particular, the mean valuation for bicycling increases. The distribution of valuations of travel time remains very close to our benchmark.

Table 21: Average estimated parameters under alternative model specifications.

Coefficients	(1)	(2)	(3)	(4)	(5)	(6)	(7)	(8)	(9)	(10)	(11)	(12)	(13)	(14)
Log(duration)	-1.92**	-1.92**	-1.79**	-1.96**	-1.92**	-2.09**	-1.92**			-1.95**	-1.74**	-1.88**	-1.91**	-1.91**
	(0.065)	(0.065)	(0.066)	(0.064)	(0.209)	(0.075)	(0.065)			(0.065)	(0.065)	(0.221)	(0.06)	(0.065)
Cost	-0.407**	-0.407**	-0.38**	-0.179**	-0.407**	-0.773**	-0.407**	-0.578**	-0.519**	-0.412**	-0.427**	-0.391**	-0.34**	-0.37**
	(0.019)	(0.019)	(0.019)	(0.012)	(0.019)	(0.036)	(0.019)	(0.021)	(0.022)	(0.019)	(0.019)	(0.05)	(0.018)	(0.019)
Duration								-0.519**	-0.97**					
								(0.018)	(0.064)					
Duration^2									0.055**					
									(0.009)					
Duration^3									-0.002**					
									(0.0004)					
Reliability			-0.103**											
			(0.015)											
Random coeff.					0.018	0.745**	-0.133							
					(0.201)	(0.059)	(0.197)							
Bicycle	-3.48**	-3.48**	-3.45**	-3.56**	-3.48**	-3.62**	-3.48**	-2.61**	-2.78**	-3.49**	-3.4**	-3.74**	-1.87**	-1.59**
	(0.082)	(0.083)	(0.082)	(0.082)	(0.449)	(0.449)	(0.449)	(0.069)	(0.072)	(0.082)	(0.082)	(0.439)	(0.055)	(0.058)
Pub. transp., peak	-4.88**	-4.83**	-5.21**	-4.73**	-4.88**	-5.28**	-4.88**	-0.808**	-0.91**	-4.85**	-4.92**	-4.62**	-5.04**	-4.82**
	(0.2)	(0.218)	(0.206)	(0.201)	(0.201)	(0.214)	(0.2)	(0.09)	(0.092)	(0.2)	(0.199)	(0.591)	(0.194)	(0.2)
Pub. transp., off-peak	-5.51**	-5.46**	-5.89**	-5.37**	-5.51**	-5.99**	-5.51**	-1.34**	-1.53**	-5.32**	-5.75**	-5.43**	-5.7**	-5.44**
	(0.403)	(0.439)	(0.412)	(0.405)	(0.404)	(0.438)	(0.404)	(0.173)	(0.189)	(0.4)	(0.398)	(1.35)	(0.393)	(0.403)
Motorcycle	-7.35**	-7.3**	-7.52**	-7.27**	-7.35**	-7.95**	-7.35**	-3.06**	-3.41**	-7.42**	-7.3**	-7.53**	-3.95**	-3.7**
	(0.226)	(0.242)	(0.232)	(0.227)	(0.67)	(0.67)	(0.67)	(0.133)	(0.139)	(0.217)	(0.215)	(0.906)	(0.11)	(0.114)
Car, peak	-6.22**	-6.16**	-6.23**	-5.48**	-6.22**	-6.78**	-6.22**	-2.05**	-2.31**	-6.18**	-6.14**	-5.94**	-6.79**	-6.15**
	(0.211)	(0.228)	(0.213)	(0.212)	(1.07)	(1.07)	(1.07)	(0.105)	(0.114)	(0.212)	(0.21)	(0.881)	(0.205)	(0.211)
Car, off-peak	-7.27**	-7.22**	-7.46**	-6.55**	-7.27**	-7.94**	-7.27**	-2.9**	-3.33**	-6.98**	-7.28**	-7.18**	-7.88**	-7.2**
	(0.214)	(0.231)	(0.216)	(0.216)	(0.214)	(0.24)	(0.214)	(0.101)	(0.119)	(0.208)	(0.209)	(0.765)	(0.211)	(0.213)
σ	0.788**	0.79**	0.86**	0.802**	0.788**	0.886**	0.785**	0.68**	0.785**	0.603**	0.561**	0.961**	0.835**	0.783**
	(0.063)	(0.063)	(0.064)	(0.063)	(0.063)	(0.075)	(0.064)	(0.053)	(0.06)	(0.049)	(0.033)	(0.116)	(0.067)	(0.062)
Log-likelihood	-13624	-13615	-13595	-13785	-13624	-13548	-13624	-13424	-13385	-13587	-15823	-14525	-14681	-13548

Note: Walk is the baseline alternative. Duration measured in minutes. Cost in €. (1): Benchmark model. (2): Weather controls. (3): Travel time reliability. (4): Car depreciation included in the cost. (5): Random coefficients on the log of duration. (6): Random coefficients on the cost. (7): Random coefficients on off-peak hour dummy. (8): Utility linear in duration. (9): Third-degree polynomial of duration. (10): alternative expected car trip durations for off-peak hours. (11): model with three periods. (12): alternative nests. (13): car available to everyone. (14): alternative definition of bicycle availability. We provide the mean coefficients, the standard-errors are computed using the delta-method.

Table 22: Values of travel time for the alternative specifications.

	Min	Q1	Mean	Median	Q99	Max
log(duration) models						
(1) Benchmark	0.442	1.34	15.9	10.3	80.6	389
(2) Weather controls	0.435	1.34	16	10.3	81.1	391
(3) Reliability measure	0.353	1.08	17.3	11.6	88.8	403
(4) Car depreciation cost	1.12	3.34	36.9	24.1	185	897
Random coefficients models						
(5) RC on log(duration)	0.44	1.35	15.9	10.3	81.1	388
(6) RC on cost	-66,161	-261	23.3	3.71	209	510,273
(7) RC on the off-peak hour dummy	0.442	1.34	15.9	10.3	80.6	389
Duration models						
(8) Duration	-0.266	-0.266	5.38	5.81	13.8	15.6
(9) 3rd degree polynomial of duration	-3.02	-2.59	52.4	15.1	477	2035
Alternative specifications						
(10) Alternative off-peak hour expected duration	0.432	1.31	17.4	11.8	87	387
(11) Model with three periods	0.211	0.75	15	9.91	78.1	335
(12) Alternative nests	0.461	1.39	17.7	12	88.2	395
(13) Car availability	0.755	1.82	21.2	13.9	101	528
(14) Bicycle availability	0.483	1.46	18.7	12.7	93.9	423

Note: in €/hr.

C.2 Additional results

VOT distribution We present the distribution of the value of travel time by age and income in Figure 6 using second-order local polynomials. Who dislikes spending time commuting thew most? Very young individuals are associated with large values of the opportunity cost of time, but the value of time decreases rapidly with age, reaching its minimum at 20 years old. After that age, the value of time increases, except for a flat part between 30 and 50 years old. The graph also indicates that the most senior individuals have the highest valuations. One of the reasons for this shape is that the estimated value of time for young children indirectly represents those of their parents, who have both to commute to work and drop off their children at school. The value of travel time rapidly decreases between 0 and 18, as older children can commute on their own to school. The steep increase afterward reflects the role of professional commitments that raise travel time value. We also see heterogeneity in the value of travel time across income categories, but the heterogeneity is much less pronounced. Poor individuals have the lowest valuations of time on average, but the opportunity cost of time increases rapidly with income. The opportunity cost of time displays an inverted bell shape. From a wealth of €360,000, the opportunity cost increases.

Figure 6: Value of travel time and individual characteristics.

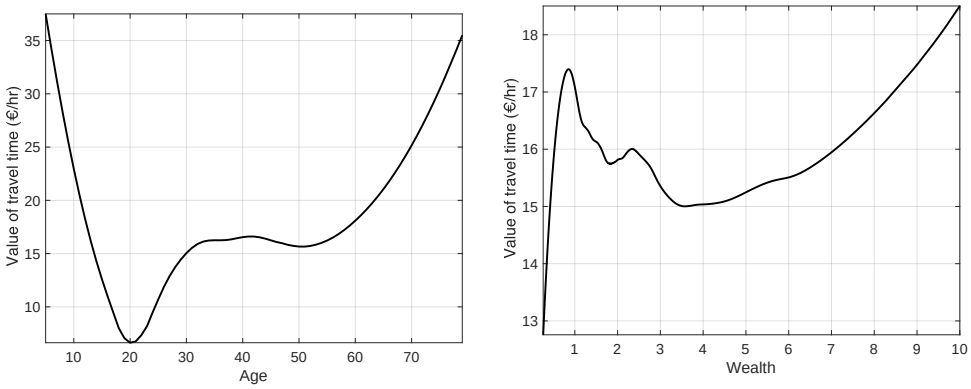

Note: Wealth is in €100,000. We winsorize values greater than 10.

Elasticities The elasticities represent the change in the probability of driving at period t when the driving duration or cost at period t' increases by 1%:

$$\mathcal{E}^{duration}_{n,t,t'} = \frac{\partial \log s_{nt}}{\partial \log \text{duration}_{nt'}} \qquad \mathcal{E}^{cost}_{n,t,t'} = \frac{\partial \log s_{nt}}{\partial \log \text{cost}_{nt'}}$$

where t and t' can be peak hour or off-peak hour.

The direct elasticities are very heterogeneous across individuals. For instance, the own duration elasticity for peak hours is between -3 and -0.06. The heterogeneity partly reflects the differences in the trip distance, which is highly correlated to duration and cost. It is also the consequence of the heterogeneity in preferences and access to efficient alternatives to cars. The cost elasticities are even more dispersed, as they are between -6.8 and 0.[34]

Individuals are less elastic to changes in duration or cost at peak hours than at off-peak hours, indicating better substitution from driving at off-peak hours to other options. The cross elasticities of driving at peak hours to the trip duration at off-peak hours are very low (0.45 on average), indicating very low substitution. The elasticity of driving at off-peak hours to the trip duration at peak hours is slightly higher, reflecting the preference for driving during peak hours. The direct elasticities to driving costs are very low, indicating that the monetary trip cost is not the most critical barrier to driving. The elasticities are slightly lower for off-peak hours than peak hours, reflecting the preference for peak hours again.

[34]We have elasticities of zero because some individuals are fully reimbursed for the driving costs by their companies, and some use electric vehicles that we assume have zero cost.

Table 23: Driving duration and driving cost elasticities.

	Min	p1%	Mean	Median	p99%	Max
Own elasticities						
$\mathcal{E}^{\text{duration}}_{\text{peak, peak}}$	-3	-2.51	-1.28	-1.29	-0.23	-0.06
$\mathcal{E}^{\text{duration}}_{\text{off-peak, off-peak}}$	-3.1	-2.66	-1.58	-1.78	-0.49	-0.43
$\mathcal{E}^{\text{cost}}_{\text{peak,peak}}$	-6.37	-2.23	-0.4	-0.22	-0.02	0
$\mathcal{E}^{\text{cost}}_{\text{off-peak, off-peak}}$	-6.78	-2.53	-0.48	-0.29	-0.02	0
Cross elasticities						
$\mathcal{E}^{\text{duration}}_{\text{peak, off-peak}}$	0.06	0.07	0.45	0.4	1.21	1.65
$\mathcal{E}^{\text{duration}}_{\text{off-peak, peak}}$	0.17	0.3	0.87	0.78	1.88	2.09
$\mathcal{E}^{\text{cost}}_{\text{peak, off-peak}}$	0	0.0009	0.13	0.08	0.73	2.42
$\mathcal{E}^{\text{cost}}_{\text{off-peak, peak}}$	0	0.006	0.21	0.13	1.23	3.88

Note: in %.

Figure 7 plots the distribution of own and cross elasticities of the probabilities of driving at peak and off-peak hours. From panel (a), we see that the elasticities at off-peak hours are higher than at off-peak hours. This implies that individuals are more likely to substitute away from driving at off-peak hours than peak hours when driving time increases, reflecting the schedule constraints. Panel (b) provides the distributions of cross-period elasticities and shows that individuals substitute more across periods when peak hour driving time changes.

Figure 7: Own and cross duration elasticities for driving.

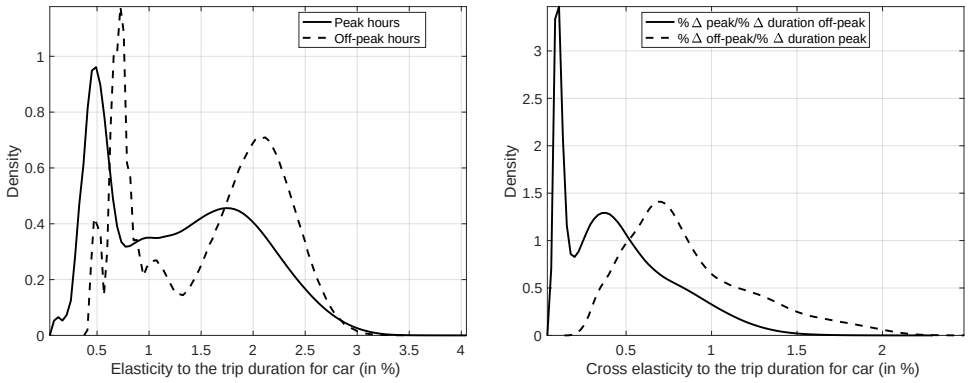

(a) Own elasticities

(b) Cross elasticities

C.3 Traffic sensor data and congestion technology estimates

C.3.1 Traffic sensor data

Data source The traffic level and speed data come from two different sources. The highway traffic data come from the regional road maintenance agency (DRIF). Traffic data for Paris

and for the ring roads come from the city of Paris.[35]

Definition of the areas Figure 8 reveals the location of the sensors (red dots) as well as the definitions of the five areas in our model: city center (light grey), ring roads (the two circles around the city center in white), the close suburb (dark grey), the far suburb (the part with no color) and the highways (the dots connecting the suburb to the city center).

Figure 8: Traffic sensors' road coverage.

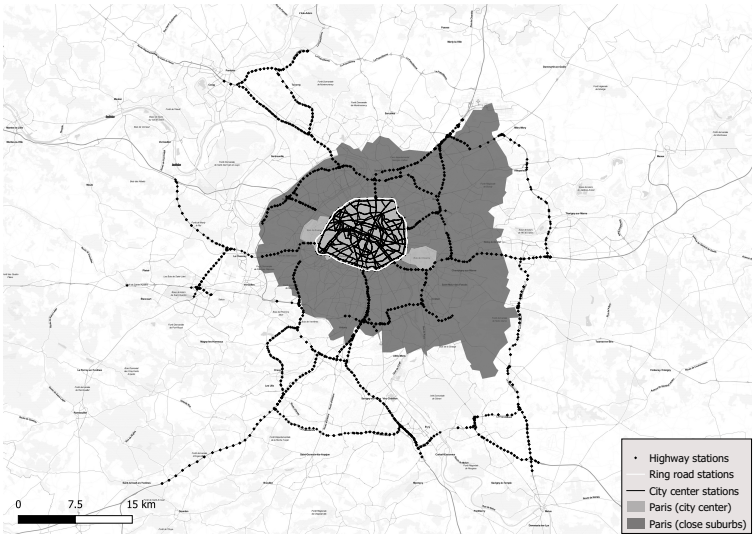

Sample construction For traffic observations from the highways connecting the far suburb to the city center, we restrict the sample to sensors that record traffic going in the direction of the city center. We drop outliers in speed (below 0 or greater than the maximum highway speed limit, 130 km/hr) and occupancy rates (below 0% and above 60%). An occupancy rate of 60% represents extreme traffic conditions: the traffic monitoring institute in Paris defines traffic as pre-saturated from 15% and saturated from 30%. We also detect inconsistent observations using the fundamental relationship between traffic flow, occupancy rates, and speed. More specifically, we combine the two equations above to get the implied average car length from traffic flow, speed, and occupancy rate:

$$\text{mean effective car length} = \frac{\text{occupancy rate} \times \text{speed} \times \text{no. lanes}}{\text{traffic flow}}.$$

We then drop observations with a car-length lower than 3.6 meters (the length of a small city car like Renault Twingo) and 18.75 meters (the size of a heavy truck). On the initial sample

[35] Source: https://opendata.paris.fr/explore/dataset/comptages-routiers-permanents-historique/information/.

of 8.9 million observations, we keep 6.2 million of them. These observations come from 654 traffic monitoring stations and constitute an unbalanced panel.

The data on the city center traffic and the ring roads contain sensor measurements of traffic flows and occupancy rates only. Unfortunately, sensors cannot measure speed accurately because of traffic lights and multiple intersections. We, therefore, estimate the speed using the formula above, but this time used to express the unobserved speeds:

$$\text{speed} = \frac{\text{traffic flow}}{\frac{\text{occupancy rate}}{\text{mean effective car length}} \times \text{no. lanes}}.$$

Instead of relying on an assumption for the effective car length as often done in the literature (e.g., Geroliminis and Daganzo, 2008 or Loder et al., 2017), we rely on the highway data to predict the average car lengths in Paris. It has been documented by Jia et al. (2001) that the traffic composition varies over time, making the uniform car length assumption inappropriate. We rely on a prediction model for the car length that we estimate using the highway data. Then, we use this model to predict hourly car lengths in the city center and the ring roads. Our prediction model specifies the mean effective car length as a function of the distance to the city center and day-of-the-week interacted with hour fixed effects. Because the relationship between the car length and the distance to the city center may not be constant as we get closer to the city center, we rely on a piecewise linear specification with six intervals. This prediction model is estimated using 4.9 million observations from highway data, for which we observe the GPS coordinates of the measurement stations and obtain an R^2 of 0.17. To predict the car length, we set the distance to the city center to 0. We then get expected car lengths specific to the hour and the day of the week. Our predictions are very realistic since they are all between 5.5 and 6.7 meters, with an average of 5.9 meters. We do not directly observe the number of lanes in the city center traffic data, so we rely on additional data from Open Street Map. Finally, we exclude outliers in occupancy rate and estimated speed following the same criteria as before for the highway data.

C.3.2 Additional results for the congestion technology estimates

Fit of the congestion technology models Table 24 represents the number of observations used to estimate the congestion technologies for each area and the fit of the models, measured by the R^2. The three congestion technologies have good fits with R^2 between 0.21 for the city center and 0.69 for the ring roads. The lower R^2 in the city center probably reflects more idiosyncrasies in traffic speed: traffic lights and intersections generate heterogeneous traffic flows, implying heterogeneous speeds.

Table 24: Fit of the congestion technology by area.

Area	Number of observations	R^2
Highways	6,195,874	0.65
City center	8,013,979	0.21
Ring roads	1,907,088	0.69

Robustness analysis We perform a sensitivity analysis to check whether the estimates of the congestion technologies are biased due to potential endogeneity issues. The concern is that some speed shocks might also affect traffic density. Such shocks may be, for example, weather conditions that change the incentives to drive (e.g., rain) and the speed (the rain may reduce visibility, so drivers slow down). To check whether our estimated congestion technologies are subject to such issues, we use hourly data on weather conditions in Paris from OpenWeather to define an extreme weather event and drop these observations. We define an extreme weather period as satisfying at least one of the following characteristics: temperature below the 5% quantile (1.39°C) or above the 95% quantile (25.28°C), a rain amount greater than the 95% quantile (0.46 mm/hr), snow or a wind speed above the 95% quantile (20.5 km/hr). We find that the estimates are robust to excluding up to 39.5% of the observations with an extreme weather condition within a three-hour window (see Figure 9).

Figure 9: Robustness checks - elimination of extreme weather conditions.

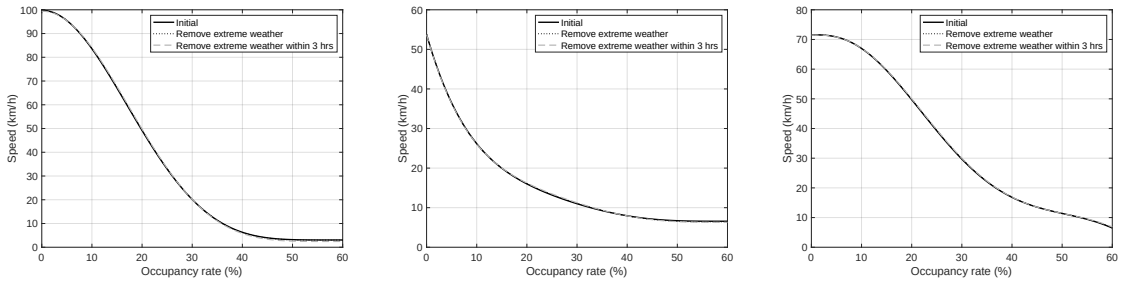

(a) Highways. (b) City center. (c) Ring roads.

Next, we may worry that road or time unobserved heterogeneity cause an endogeneity problem for the estimation of the congestion technologies. To check this, we allow the congestion technologies to vary across stations or time. More specifically, we estimate congestion technologies by subgroup and then aggregate them to construct an average congestion technology. Since we approximate the speed functions by Bernstein polynomials of order seven we can only consider subgroups with more than eight observations. The aggregate congestion technologies are displayed in Figure 10. We see that adding road or time heterogeneity do not substantially change the shapes of the congestion technologies.

Figure 10: Robustness checks - congestion technologies estimated by subgroups.

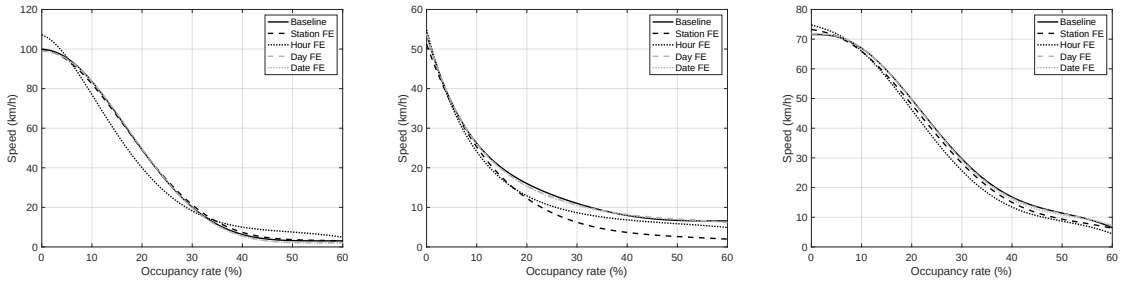

(a) Highways. (b) City center. (c) Ring roads.

C.3.3 Additional results for mapping between individual decisions and road traffic levels

We evaluate the model's fit by comparing the aggregate frequency of each transportation mode observed in the data with the predicted frequency from our model. Table 25 below shows the observed and predicted shares. The difference between Columns 1 and 2 comes only from the winsorizing of a few speed shock outliers (below 1/2 or above 2). The trimming has virtually no impact on the predicted shares. In column 3, we solve for the equilibrium speeds and individual choices using the full model. Since we calibrate the mapping parameters by imposing constraints, we do not exactly match the initial occupancy rates. However, our model predicts transportation mode shares close to the observed shares.

Table 25: Shares of transportation modes observed and predicted by the model.

	Observed	**Predicted initial speeds**	**Predicted full model**
Bicycle	2.1	2.1	2.09
Pub. transport, peak	30.3	30.3	30.3
Pub. transport, off-peak	14.5	14.6	14.6
Motorcycle	2.08	2.08	2.08
Walking	15.8	15.8	15.8
Car, peak	22.9	22.8	22.9
Car, off-peak	12.3	12.3	12.3

Note: in %.

Table 26 shows the comparison between the average speeds from traffic data and those predicted from the model equilibrium. Our estimates are optimistic for the highways at peak hours but pessimistic for ring roads and the city center. We nevertheless correctly predict the speeds ranking between areas for both periods.

Table 26: Predicted equilibrium speeds and average speeds from traffic data.

	Peak hour		Off-peak hour	
Area	**Traffic**	**Eq. speeds**	**Traffic**	**Eq. speeds**
Highways	44.9	65.2	67	85.4
City center	22.4	13.7	31.7	18.3
Ring roads	30.4	28.8	57.9	44.2
Close suburb		15.8		20.2
Far suburb		25.5		29.2

Note: in km/hr.

C.4 Additional results on the equilibrium solving algorithm

We show additional numerical results about the convergence by plotting the average number of iterations needed to converge for the possible values of κ between 0.45 and 0.95. More specifically, we draw 10 different initial speed values from a uniform distribution over $[\underline{\mathbf{v}}, \overline{\mathbf{v}}]$ and solve for the speed equilibrium with different values for the tuning parameter. As expected, the number of iterations and the time increases exponentially from $\kappa = 0.45$ onward. Furthermore, we always converged to the same equilibrium speeds regardless of the policy environment. This shows that the choice of setting $\kappa = 0.5$ is efficient in terms of speed of convergence.

Figure 11: Average number of iterations and convergence times (across 10 simulations).

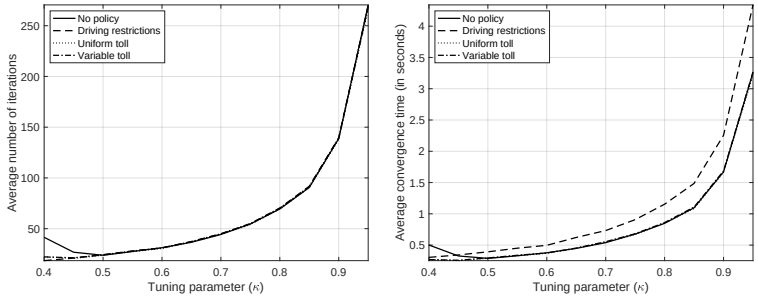

(a) Number of iterations. (b) Average convergence time.

D Additional results on the policy effects

D.1 Consumer surplus and welfare definitions

To evaluate the impacts of transportation policies on individuals, we rely on changes in consumer surplus, which measure compensating variations. The consumer surplus per trip for

individual n is defined as the expected utility of the choice that maximizes the utility and is:

$$CS_n = \frac{1}{|\alpha_n|} \log \left(\sum_{j \in \mathcal{J}_n} \exp(\sigma \log(D_{nj})) \right) + C_n,$$

where $D_{nj} = \sum_{t=1}^{T} \exp\left(\frac{\beta_n' X_{njt}}{\sigma}\right)$ is the expected utility of the best departure period for transportation mode j. C_n represents a constant utility term that cannot be identified, and α_n is the parameter of sensitivity to the trip cost, which converts the utility into monetary terms. The consumer surplus level is not identified, but the variation of consumer surplus eliminates the constant C_n and thus is identified and given by:

$$\Delta CS_n = \frac{1}{|\alpha_n|} \left[\log \left(\sum_{j \in \mathcal{J}_n^1} \exp(\sigma \log(D_{nj}^1)) \right) - \log \left(\sum_{j \in \mathcal{J}_n^0} \exp(\sigma \log(D_{nj}^0) \right) \right].$$

Where $\mathcal{J}_n^1$ and D_{nj}^1 represent respectively the choice set and the expected utility of transportation mode j under the counterfactual scenario, while $\mathcal{J}_n^0$ and D_{nj}^0 represent their initial values. We can further decompose the variation in consumer surplus into a partial policy effect which measures the policy effect at constant initial speeds, and an equilibrium speed effect under the implemented policy. To make the expression clearer, we make apparent the dependence between the driving speeds and the utilities associated with the transportation modes $D_{nj}^0(\mathbf{v_0})$ and $D_{nj}^1(\mathbf{v_1})$, where $\mathbf{v_0}$ and $\mathbf{v_1}$ represent the initial and final vectors of speeds. The decomposition is given by:

$$\begin{aligned}\Delta CS_n = \frac{1}{|\alpha_n|} \Bigg[& \underbrace{\log \left(\sum_{j \in \mathcal{J}_n^1} \exp\left(\sigma \log\left(D_{nj}^1(\mathbf{v_0})\right)\right) \right) - \log \left(\sum_{j \in \mathcal{J}_n^0} \exp\left(\sigma \log\left(D_{nj}^0(\mathbf{v_0})\right)\right) \right)}_{\text{policy effect at constant speed}} \\ & + \underbrace{\log \left(\sum_{j \in \mathcal{J}_n^1} \exp\left(\sigma \log\left(D_{nj}^1(\mathbf{v_1})\right)\right) \right) - \log \left(\sum_{j \in \mathcal{J}_n^1} \exp\left(\sigma \log\left(D_{nj}^1(\mathbf{v_0})\right)\right) \right)}_{\text{equilibrium speed effect}} \Bigg]\end{aligned}$$

The total consumer surplus change is then obtained by summing individual surplus changes over individuals.

We consider two welfare measures. The first is simply the sum of consumer surplus change

and the potential toll revenue:

$$W_1 = \sum_{n=1}^{N} \omega_n \left(\Delta CS_n + \sum_{j \in \mathcal{J}_n^1} \sum_{t=1}^{T} \mu_{njt} s_{njt}^1 \right),$$

where μ_{njt} is the toll for individual n, transportation mode j and period t, and s_{njt}^1 represents the transportation mode choice probability under the counterfactual policy. We consider a second welfare measure which includes consumer surplus change, tax revenue, and the change in emissions valued at standard levels:

$$W_2 = \sum_{n=1}^{N} \omega_n \left(\Delta CS_n + \sum_{j \in \mathcal{J}_n^1} \sum_{t=1}^{T} \mu_{njt} s_{njt}^1 + \sum_{j \in \mathcal{J}_n^1} \sum_{t=1}^{T} \lambda_{njt} \left(s_{njt}^1 - s_{njt}^0 \right) \right),$$

where λ_{njt} represents the cost of emissions for individual n, transportation mode j and period t.

D.2 Importance of endogenous speeds

In Figure 12, we compare our model's predictions for car shares with those from a naive model that would consider speeds and trip durations fixed. All scenarios and stringency levels deliver the same biases under exogenous speeds: we overestimate the number of individuals substituting away from using their cars at peak hours and underestimate those who choose to drive at off-peak hours. The equilibrium speed effects indeed dampen incentives to stop driving.

Figure 12: Predicted car shares as function of the policy stringency level.

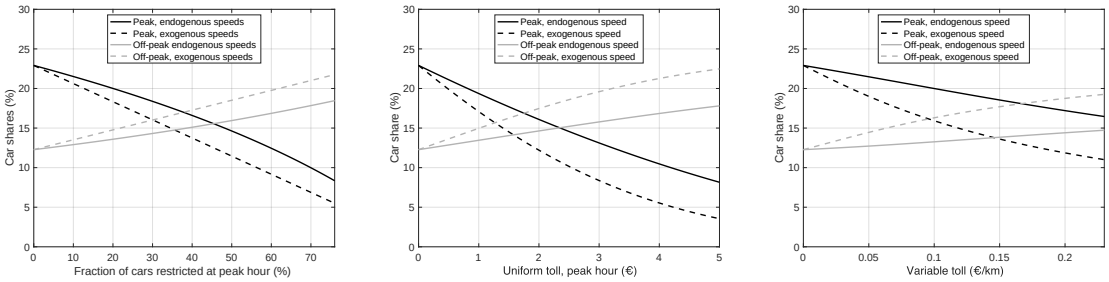

(a) Driving restrictions. (b) Uniform tolls. (c) Variable tolls.

We provide the equilibrium speeds for three areas for all policy stringency levels in Figure 13. At peak hours, the speeds increase with the policy stringency level, while at off-peak hours, they decrease monotonically. This is the consequence of major shifts towards driving at off-peak hours. The speed at peak hours changes the most on the highways while there is

much less speed improvement in the city center. At the same time, the off-peak hour speed in the city center is almost constant. This reflects that individuals driving in the city center have better alternatives to cars, while those who use the highways and the ring roads are more likely to substitute for driving during off-peak hours.

Figure 13: Speeds under the different policies and stringency levels.

Peak hours.

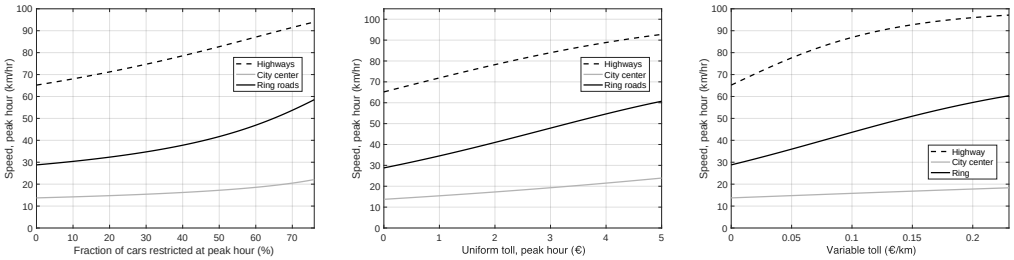

(a) Driving restrictions. (b) Uniform tolls. (c) Variable tolls.

Off-peak hours.

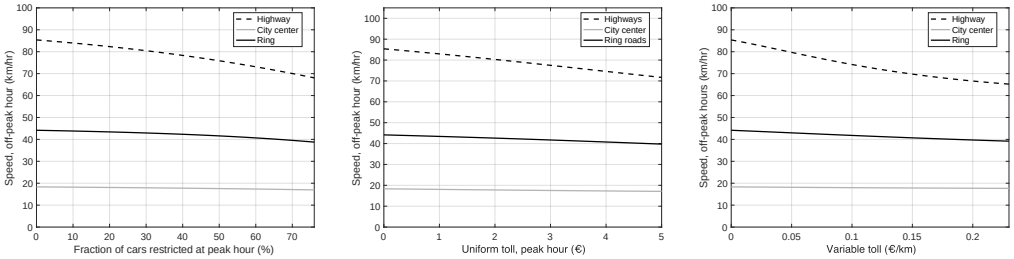

(d) Driving restrictions. (e) Uniform tolls. (f) Variable tolls.

To further highlight the importance of taking into account the equilibrium speed adjustments, we compare the tax revenues predicted under constant speeds with the predictions from our model. The results, in Figure 14 below, suggest that not accounting for the changes in speeds significantly underestimates the number of individuals paying the toll and the tax revenue. Moreover, the magnitude of the bias increases with the policy stringency levels, reflecting the increasing role of speed adjustments. In addition, we note that the tax revenues follow a Laffer curve under both toll types and decrease when the toll levels are too high. This maximum level is attained more rapidly for the uniform toll than the variable.

Figure 14: Predicted tax revenues under tolls at peak hours.

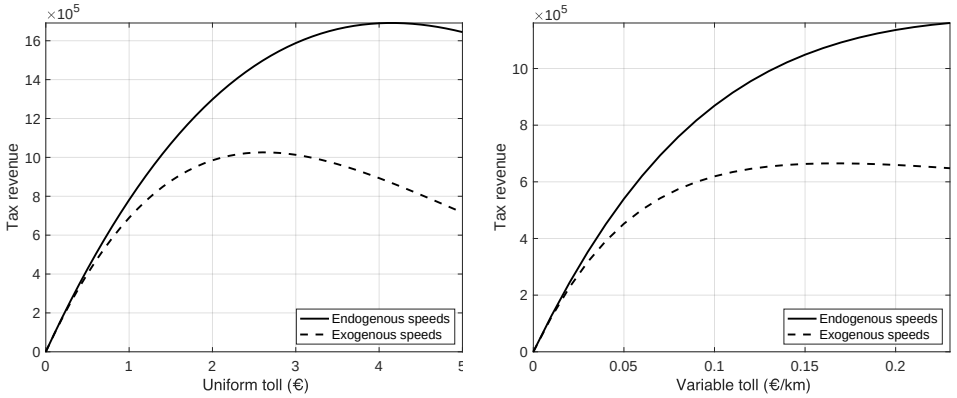

(a) Uniform tolls.

(b) Variable tolls.

D.3 Additional results for the benchmark policy levels

Modal shift The aggregate shares of transportation modes are reported in Table 27. They indicate a significant inter-temporal modal shift towards driving at off-peak hours. The share of car users at peak hours drops under all policies, but the magnitudes differ. For example, while driving restrictions and uniform tolls decrease the number of car users by 8.3 to 8.9 percentage points, the variable toll only decreases it by 2.9 percentage points. This is because the variable toll discourages individuals with long distances from driving and keeps the number of drivers relatively high. For the same reason, we also observe essential differences in the modal shifts across policies: driving restrictions and the uniform toll increase the fraction of individuals who walk and take public transport more than the variable toll.

Table 27: Predicted shares of the transportation modes under different policies.

	Initial	**Driving restriction**	**Uniform toll**	**Variable toll**
Bicycle	2.09	2.3	2.34	2.09
Pub. transport, peak	30.3	32.2	32.7	31.4
Motorcycle	2.08	2.44	2.49	2.31
Walk	15.8	17.1	17.4	15.8
Car, peak	22.9	14.6	14	20
Car, off-peak	12.3	15.9	15.4	13.3
Pub. transport, off-peak	14.6	15.4	15.6	15.1
Total car share	35.2	30.6	29.4	33.2
Total pub. transport share	44.8	47.5	48.3	46.6

Note: in %.

Impacts on individual trip durations We complement the analysis by looking at how the policies impact the expected travel times in Table 28 below. There is an enormous

difference in the total travel time increase across policies: under the variable toll, it is only 2.3 thousand hours against 25 to 29 thousand hours under the uniform toll and the driving restriction. This reflects the extensive substitution for driving at off-peak hours under the variable toll. It further indicates that the surplus losses from the variable toll are mainly related to the surplus loss from driving outside peak hours and paying high tolls than an increase in travel time. The distribution of changes in travel time under all policies is skewed towards more extensive trips. For instance, the maximum time reductions are always lower than the maximum increases in travel time. This skewness is more pronounced under the variable toll, associated with a maximal duration increase of 41 minutes versus 24 to 27 minutes for the two other policies. Under the three policies, some individuals reduce their expected trip durations. The variable toll has the largest share of individuals with reduced travel times, with 56% of the individuals versus 28% and 29% under the two other policies.

Table 28: Trip duration variation under alternative policies.

	Driving restriction	**Uniform toll**	**Variable toll**
Min Δduration	-10.4	-13	-10.9
Mean Δduration	0.371	0.423	0.034
Max Δduration	24.4	26.9	40.5
Total Δduration (in 1,000 hrs)	24.9	28.5	2.32
% Δduration > 0	50.4	51.9	23.7
% Δduration < 0	29.3	27.9	56

Note: Δ durations are in minutes, except "Total Δ duration".

Speed changes We analyze the speed changes for the different areas in Table 29. The variable toll most improves the speed on the highways at peak hours. The variable toll is also better than the driving restriction to improve the speed on the ring roads at peak hours. However, it raises speeds in the city center and the suburbs the least at peak hours. This occurs because the individuals who drive on the highways and ring roads have long distances and are discouraged from using their cars at peak hours. But since they do not have good transportation alternatives, they drive during off-peak hours. This is consistent with the highest speed reduction at off-peak hours under the variable toll. The uniform toll is the policy that enhances the speeds at peak hours in the city center, the ring roads, and the close suburb the most. Across the three regulations, the area with the smallest improvements is the far suburbs, revealing a lack of good car alternatives. For instance, public transport offers poor coverage in the distant suburb. The speeds at off-peak hours decrease in all areas but remain higher than the initial levels at peak hours. This reflects the imperfect substitution between driving at peak and off-peak hours, which avoids having a simple shift of the peak hour period.

Table 29: Predicted speeds under the different policies.

	Area	Initial	Driving restriction	Uniform toll	Variable toll
Peak hours	Highways	65.2	82.7	82.3	87
	City center	13.7	17.2	18.6	15.8
	Ring roads	28.8	41.7	45.7	43.7
	Close suburb	15.8	19.6	20.4	17.9
	Far suburb	25.5	28.4	28.2	27.6
Off-peak hours	Highways	85.4	75.9	78.4	74.1
	City center	18.3	17.6	17.6	18
	Ring roads	44.2	41.6	42	41.8
	Close suburb	20.2	18.8	18.9	19.6
	Far suburb	29.2	27.1	27.5	27.7

Note: in km/hr.

Marginal costs of congestion Table 30 presents the marginal congestion costs for each area and period under the different policies. We provide the marginal costs associated with adding one average driver in each area to account for differences in area sizes. The driving restriction and uniform toll reduce the marginal congestion costs across all areas at peak hours. However, we observe an increase in the marginal costs of congestion in the city center and the close suburb at peak hours under the variable toll. The cost increases are lower than 8%, and we can observe the opposite pattern at off-peak hours, where the costs decrease in the same two areas and the far suburb. This occurs because the speed improvements make individual trip durations lower, increasing and in turn increase their marginal valuations of duration. Thus, having an additional driver on the road raises the surplus losses for individuals. The marginal costs on the highways and the ring roads are the most reduced by the policies.

Table 30: Marginal costs of congestion under the different policies.

	Area	Initial restriction	Driving toll	Uniform toll	Variable
Peak hours	Highways	1.14	0.493	0.507	0.412
	City center	1.58	1.35	1.3	1.7
	Ring roads	2.09	1.29	1.09	1.3
	Close suburb	1.29	1.07	1.04	1.39
	Far suburb	0.582	0.394	0.403	0.575
Off-peak hours	Highways	0.415	0.753	0.662	0.762
	City center	1.26	1.3	1.3	1.19
	Ring roads	1.19	1.31	1.29	1.22
	Close suburb	1.04	1.12	1.12	0.975
	Far suburb	0.339	0.509	0.486	0.39

Note: costs associated to adding an average driver, in €.

D.4 Differentiated tolls

This section investigates the consequences of applying differentiated tolls. First, we study the welfare-maximizing personalized tolls. Second, we consider tolls that depend on the areas where individuals drive. Finally, we analyze combinations of fixed and variable tolls.

Welfare-maximizing personalized tolls In addition to comparing benchmark policy levels, we investigate the gains from welfare-maximizing personalized tolls for any traffic level achieved. Figure 15 below shows the variation in aggregate welfare relative to the initial equilibrium for any traffic reduction level under personalized tolls. We observe that the optimal traffic reduction is slightly below the one achieved with a variable toll.

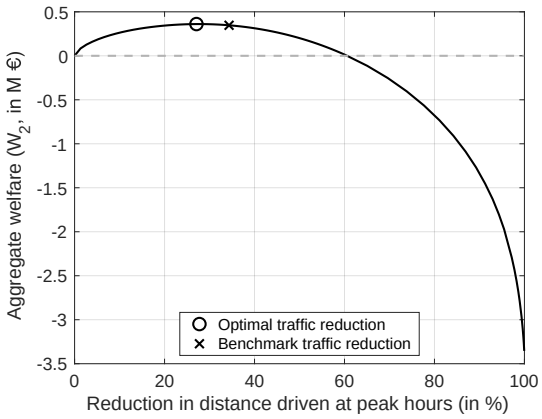

Figure 15: Welfare changes from personalized tolls maximizing W_2.

Area-specific tolls We consider a toll that takes two different values: one for the city center and ring roads and one for the highways and the close and far suburbs. This policy instrument is similar to a cordon pricing mechanism. We determine all the toll combinations that imply the same objective traffic at peak hours and find the best toll combination for different objectives. When individuals drive through the two toll zones, we assume they only pay the highest toll.[36] Area-specific tolls might incentivize individuals to change their route choice. Still, we believe that the relatively large definition of areas in our setup considerably limits this potential effect.

The left graph in Figure 17 shows all the combinations of road tolls that achieve the same objective traffic at peak hours. The right graph in Figure 16 provides the change in

[36] Alternatively, we could assume individuals driving through the two toll areas pay the sum of the tolls, but this situation would not nest the benchmark uniform toll.

total welfare (measured by the sum of consumer surplus and tax revenue minus the cost of emissions) for different toll values in the suburb. First, the uniform toll is not too far from the tax revenue-maximizing toll combination. The welfare is maximized for the combination of €2.15 in the suburb and €4.06 in the city center; it multiplies the total welfare gain from the uniform toll by two. We also provide the toll values that maximize consumer surplus (both with and without redistributive weights); they set a low toll value in the suburb (€1) and a high value of €14.7 inside the city center.

Figure 16: Differentiated tolls and their welfare impacts.

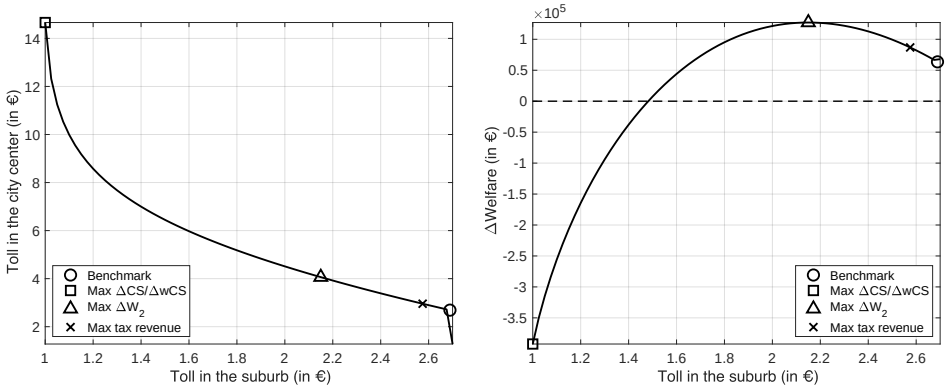

(a) Toll combinations.

(b) Welfare (W_2).

Combination of fixed and variable tolls We now consider another way to define tolls, given by a fixed and a variable part. We allow for negative values of the two components of the toll. Interestingly, the best toll value for consumer surplus has the lowest fixed and highest variable parts. This means that individuals receive a fixed amount when taking their car but pay a high fee for each kilometer driven. Since individuals with short trips have higher valuations of travel time than individuals with more extended trips, their gains largely compensate for the losses of long-distance commuters and their high toll values, achieving the maximum aggregate surplus. However, this combination of road tolls is not efficient at raising tax revenue. This is why the best combination, from a welfare perspective (defined as the sum of the aggregate surplus and the tax revenue minus the costs of emissions), is a toll with a smaller variable part than our benchmark variable toll (7 cents/km instead of 9 cents/km) and a moderate fixed amount of €0.73. This toll combination would improve the welfare gains by 13.3%. We could reach the maximum tax revenue with the high fixed value of €3.2 and a negative variable part (-0.2 cents/km). This combination of tolls would however be welfare-decreasing, as Figure 17 (b) suggests.

Figure 17: Combination of fixed and variable tolls and their welfare effects.

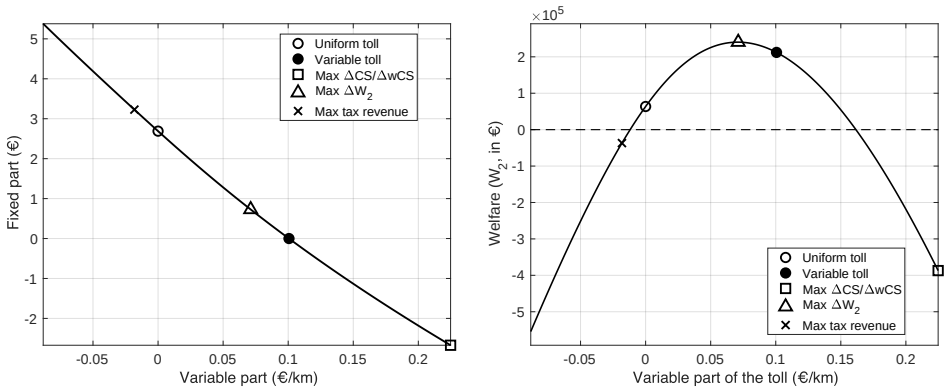

(a) Toll combinations.

(b) Welfare (W_2).

D.5 Auctioned driving license

We consider a simple uniform second-price auction format, which implies that individuals bid their true license valuation. The equilibrium price is the highest rejected bid associated with a fixed number of licenses. Individual valuations are equal to the difference between the expected utilities with and without the right to drive, and we assume individuals perfectly anticipate the speed improvements. However, they do not know their preference shocks before submitting their bids. Thus, the willingness to pay includes the gain in utility from better speeds at peak hours. We use an iterative algorithm to solve for the license price together with the equilibrium speeds for a given quota of driving licenses. Our algorithm cannot find a stable equilibrium for some values of the quota of driving licenses. This occurs when we consider stringent policies (i.e., with a low number of permits) where the speed gains are significant. We thus select the quota of driving licenses that implies the closest outcome to the one obtained in our main policies. Then, we re-calibrate the uniform toll to match the traffic reduction across policies. We thus analyze policies that are milder than before since they trigger a decrease in traffic at peak hours of 25.2%. This policy seems more suited to a comparison with the uniform toll, as they both put a price on the right to drive. However, there is an essential difference from the perspective of individuals. Under the toll, individuals decide to drive and pay the toll after they receive their preference shocks for the transportation modes and departure times. While under the auction, individuals have to submit their bid for the license before receiving their preference shocks and lose the ability to react in case of extreme preference shocks. We provide the policy parameters in Table 31 below. We find a uniform toll of €1.89, higher than the license price of €1.30. Since individuals do not know their mode and departure period preference shocks when bidding,

they have moderate valuations for the driving license.

Table 31: Parameters for the driving license quota and equivalent uniform toll policies.

Policy type	**Parameter**	**Value**
License	Quota of licenses	31.1%
	License price	1.30
Uniform toll	toll	1.89

Note: License price and toll in €/trip.

Since individuals who get the license pay for it regardless of how often they decide to drive at peak hours, the policy generates considerably higher surplus losses. Individuals can no longer react to good or bad realizations of their preference shocks for driving. Indeed, the driving license regulation causes 66% more surplus losses than the uniform toll. The two policies generate comparable tax revenue of around €1.3 million. Under tax revenue redistribution, the quota of driving licenses causes a net welfare loss of €0.6 million, while the uniform toll is welfare enhancing.

However, we can see that the driving license quota is more effective than the toll to reduce emissions: we obtain 54% more reduction in CO_2 emissions and 58% more reduction in emissions of local pollutants. Despite the important environmental effect, once converted in monetary terms, the emissions gains do not offset higher surplus losses from the quota of licenses since our second welfare measure is also higher under the uniform toll. Both with and without the redistribution of the tax revenue, the average cost of reducing emissions is lower under the uniform toll. From a distributional point of view, both policies seem to have similar effects, generating identical shares of losers and virtually no winners. The total consumer surplus losses are very similar with or without the redistributive weights, indicating that the driving license quota is not a regressive regulation.

Table 32: Driving license versus uniform toll.

	Uniform toll	**License**
Total ΔCS (M€)	-1.14	-1.9
ΔCS, constant speed	-1.37	-0.997
ΔCS from speed	0.23	-0.907
Total ΔwCS (M€)	-1.18	-1.95
Tax revenue (M€)	1.28	1.31
ΔW_1 = ΔCS + Tax revenue (M€)	0.142	-0.592
ΔW_2 = ΔCS + tax rev. - ΔE (M€)	0.169	-0.55
ΔCO_2 (ton)	-285	-440
$\Delta eqNO_X$ (ton)	-1.19	-1.88
Implied cost local pollutants (€/ton NO_X)		
Without redistribution	956,790	1,015,204
With redistribution	-119,543	315,530
% ΔCS > 0	0	0.133
% ΔCS < 0	79.7	79.6

Note:"ΔE" are changes in emissions valued at standard levels.

D.6 Robustness checks for the policy simulations

D.6.1 All-day policies

In this section, we analyze the impacts of policies applied during the whole day. As before, we first apply driving restrictions with a probability of 0.5 and then calibrate the uniform and variable tolls to obtain the same total traffic reduction. This time the traffic is calculated by the sum of kilometers driven at peak and off-peak hours. The parameters are provided in Table 33 below and show that the tolls are much larger than when the policies are applicable at peak hours only. Since 4.06% of the individuals in our sample do not have an alternative to cars, we allow them to be non-compliant to the regulation. In exchange, they pay a fee of €68. This value is inspired by the fine for breaking the driving restriction rule applied to Paris in 2016. This value is also a proxy for the cost of using a taxi instead of the driver using their own car. We only allow those without alternatives to be non-compliant in the main analysis.

Table 33: All-day policy parameters.

Outcome matched	**Driving restriction**	**Uniform toll**	**Variable toll**
Distance, peak and off-peak hours	50%	4.26	0.20

Note: Uniform toll in €, and variable toll in €/km.

Modal shifts Table 34 presents the predicted shares for each transportation mode under the different policies. Under such strict regulations, we observe significant modal shifts away from cars toward other transportation modes. The variable toll implies more substitution for public transport and less substitution for walking than the other policies. This is because variable tolls discourage individuals with long commutes, who typically cannot walk to work.

Table 34: Predicted shares of the transportation modes under all-day policies.

	Initial	**Driving restriction**	**Uniform toll**	**Variable toll**
Bicycle	2.09	3.82	2.65	2.11
Pub. transport, peak	30.3	35.3	36.5	34.2
Motorcycle	2.08	3.1	3.26	2.97
Walk	15.8	19.6	19.1	16
Car, peak	22.9	14.1	13.9	19.1
Car, off-peak	12.3	6.92	6.95	9.14
Pub. transport, off-peak	14.6	17.2	17.7	16.6
Total car share	35.2	21	20.8	28.2
Total pub. transport share	44.8	52.5	54.2	50.8

Note: in %.

Welfare impacts Table 35 shows the welfare impacts of the three all-day policies. Surplus losses from all-day policies are considerably higher than from peak-only policies. These results highlight the effect of closing the inter-temporal substitution channel that allows individuals to keep driving. These strict policies decrease the total consumer surplus by €2.8 million to €7 million, depending on the type of policy in place. We specifically observe exceptionally high losses from driving restrictions, but this is linked to the fine for non-compliance. This policy raises €3.4 million from the non-compliance penalties. As before, we find differences in the tax revenue raised by the different policies. The uniform toll collects more toll payments than the variable toll. Yet, the tax dividend does not compensate for the surplus losses like under the peak-hour uniform toll.

We can also observe that strict policies are much more effective at reducing emissions than the mild policies, applied at peak hours only. Indeed, the strict regulations lead to at least three times more reduction. As a consequence, the welfare measures increase by roughly €0.1 million when we include the values of emission reductions. We find that the average cost ranking of the policies is the same as before: we obtain very high costs for driving restrictions but reasonable costs for the uniform tolls.

Table 35: Consumer surplus variation under all-day policies.

	Driving restriction	**Uniform toll**	**Variable toll**
Total ΔCS (M€)	-6.44	-3.74	-2.57
ΔCS, constant speed	-7.07	-4.38	-3.26
ΔCS from speed	0.638	0.642	0.696
Total ΔwCS (M€)	-7.01	-3.92	-2.8
Tax revenue (M€)	3.43	3.58	2.82
ΔW_1 = ΔCS + tax revenue (M€)	-3.01	-0.159	0.257
ΔW_2 = ΔCS + tax rev. - ΔE (M€)	-2.91	-0.058	0.357
% ΔCS > 0	0.075	0	11.9
% ΔCS < 0	79.7	79.7	67.8
Δ CO_2 (ton)	-1,055	-1,067	-1,055
Δ eqNO_X (ton)	-4.43	-4.47	-4.41
Implied cost CO_2 (with redist)	2,849	149	-244
Implied cost eqNO_X (with redist)	678,669	35,621	-58,243

Note: "ΔE" are changes in emissions valued at standard levels.

D.6.2 Increase in public transport overcrowding

We compare the benchmark variable toll and two scenarios where the policy is followed by a 15% or a 30% increase in the overcrowding levels in public transport. Table 36 presents the impact of these policies on consumer surplus and aggregate welfare. In the two scenarios, the total surplus loss would be 9% and 18% higher, highlighting the limited role of public transport overcrowding. Moreover, tax revenues remain almost constant under the three scenarios since

the share of individuals driving is barely affected by the change in the overcrowding level. Finally, the welfare outcomes decrease by between 28% and 66%, mainly because of the larger surplus losses. Yet, we still obtain a positive effect from the variable toll.

Table 36: Policy effects with overcrowding level changes in public transit.

	Overcrowding constant	**Overcrowding +15%**	**Overcrowding +30%**
Total ΔCS (M€)	-0.691	-0.754	-0.817
ΔCS, constant speed	-0.931	-0.986	-1.04
ΔCS from speed	0.24	0.232	0.224
Total ΔwCS (M€)	-0.752	-0.812	-0.872
Tax revenue (M€)	0.872	0.875	0.877
Δ W_1 = ΔCS + Tax revenue (M€)	0.181	0.12	0.06
ΔW_2 = ΔCS + tax rev. - ΔE (M€)	0.212	0.151	0.09
Δ CO_2 (ton)	-330	-322	-313
Δ eqNO_X (ton)	-1.37	-1.34	-1.31

Note: "ΔE" are changes in emissions valued at standard levels.

D.6.3 Change in travel time reliability

We study the robustness of our policy effect predictions by including the sensitivity to travel time reliability in the transportation choice model. To do so, we take the model parameters in Column (3) of Table 21 in Appendix C.1 and measure the impacts of the benchmark variable toll. We modify the reliability values in the following way: the standard deviation of travel time decreases by 46.5% for everyone at peak hours while it increases by 11.9% at off-peak hours. These values correspond to the maximum percentage speed increase in an area for peak hours and the maximum speed decrease for off-peak hours. We believe these values correspond to an extreme case with large changes in reliability levels. What we do here is different from considering reliability an equilibrium outcome, but it is informative on the importance of endogenizing reliability for the welfare results.

Table 37 shows the predicted shares for each transportation mode. Across the different scenarios, we see that including reliability and modifying its value have little impact on the predicted shares for the different transportation modes. The inclusion of reliability increases car usage at peak hours by less than 1%. These results suggest that the role of travel time reliability is limited for individual transportation decisions.

Table 37: Shares of transportation modes under the variable toll with different reliability scenarios.

Mode	Benchmark	Constant reliability	Updated reliability
Bicycle	2.09	2.09	2.09
Pub. transport, peak	31.4	31.3	31.1
Pub. transport, off-peak	15.1	15.1	15
Motorcycle	2.31	2.29	2.26
Walk	15.8	15.8	15.8
Car, peak	20	20.3	20.8
Car, off-peak	13.3	13.1	12.9
Total car	33.2	33.4	33.8
Total pub. transport	46.6	46.4	46.1

Note: for 'updated reliability', the standard deviation of travel time decreases by 46.5% at peak hours and it increases by 11.9% at off-peak hours.

Table 38 presents the welfare impacts of the variable toll with and without accounting and updating the reliability measures. Overall, the aggregate surplus changes remain in the same order of magnitude. The difference in results between our benchmark and the model with constant reliability comes from the fact that we use different sets of demand parameters. These differences are not excessive, indicating that the two models do not deliver very different policy predictions. More relevant to understanding the value of improved reliability is to compare the welfare effects of the variable toll under constant reliability and the model where we update the values of travel time reliability. We see a net surplus gain from improved reliability at peak hours evaluated at €0.09 million. This scenario also results in a larger tax revenue since more individuals prefer paying the toll for the improved speeds and reliability at peak hours. In the end, we estimate a net benefit of the variable toll to be €0.42 million, which is 50% higher than without the improvement in reliability at peak hours. Improving reliability increases the share of winners by only 2.7 percentage points.

Table 38: Consumer surplus variation from variable tolls under different reliability scenarios.

Mode	Benchmark	Constant reliability	Updated reliability
Total ΔCS (M€)	-0.691	-0.617	-0.532
ΔCS, constant speed	-0.931	-0.82	-0.725
ΔCS from speed	0.24	0.203	0.193
Total ΔwCS (M€)	-0.752	-0.668	-0.584
Tax revenue (M€)	0.872	0.876	0.935
ΔW_1 = ΔCS + Tax revenue (M€)	0.181	0.259	0.402
ΔW_2 = ΔCS + tax rev. - ΔE (M€)	0.212	0.288	0.427
% ΔCS > 0	18.9	15.4	18.1
% ΔCS < 0	60.8	64.4	61.6

Note: for 'updated reliability', the standard deviation of travel time decreases by 46.5% at peak hours and it increases by 11.9% at off-peak hours. "ΔE" are changes in emissions valued at standard levels.